PLASMA RESEARCH

CASE INSTITUTE OF TECHNOLOGY

[redacted]

UNIVERSITY CIRCLE • CLEVELAND 6, OHIO

Development of Lasers for Plasma Diagnostics

by

W. B. Johnson

T. P. Sosnowski

Technical Report No. A - 29

July, 1964

* Support received in part by the Case Institute of Technology Research Fund and the National Aeronautics and Space Administration.

ACKNOWLEDGEMENTS

The authors would like to express their thanks to the many members of the staff of Case Institute of Technology who contributed greatly to this work. Particularly helpful were Mr. Harlan Cook, whose technical assistance greatly facilitated the work in the laser laboratory, and Mr. Ed Parillo and Mr. Imre Szilagyi, the glass blowers, whose skills were indispensable in the construction of the laser tubes. Finally, we are grateful to the Case Institute of Technology Research Fund and the National Aeronautics and Space Administration for financial support of this project.

ABSTRACT

11738

This report deals with the construction of an optical heterodyne system for the purpose of measuring the electron density of a plasma. Initially the plausability of the scheme is established theoretically. This is followed by a detailed account of the construction of the helium-neon gaseous lasers necessary for the project. Design parameters are established to determine the most efficient means of operation of the laser for the proposed experiment. It is found that the laser can operate at gas pressures and input currents from 1.6 mm to greater than 10 mm Hg pressure and 5 ma to greater than 60 ma respectively, with optimum operation occurring at 3.8 mm Hg pressure at a current of 30 ma. The heterodyning of two laser beams is then considered; the stability of the resultant beat frequency is found to be seriously impaired by such environmental factors as building vibration and very small temperature fluctuations. The minimum frequency drift encountered in the experiment was approximately 50 kc/s in a 1 sec period and is comparable to the frequency shift obtained with an electron density of 10^{12} electrons/cc. Recommendations are then made which should to a great extent either mitigate or eliminate the causes of frequency drift.

Author

TABLE OF CONTENTS

Chapter

LIST OF ILLUSTRATIONS

CHAPTER I

INTRODUCTION

1.1 Purpose of the Thesis

The potential of the laser as a diagnostic tool in various fields of science has been clearly recognized since its advent in 1960. Inherent properties such as coherence and monochromaticity make it an ideal instrument for the study of, among other things, ionized gases or plasmas. In the plasma dynamics department of this institution, a proposal was made to investigate the electron densities of a plasma with a laser system. Essentially the system is an optical heterodyne device utilizing two lasers; one has its frequency changed by the action of the plasma, and the other acts as a reference frequency. It is possible then, by comparing the difference in frequency between the two lasers, to determine the absolute shift in frequency of the laser under the influence of the plasma. It was determined that a continuous wave helium-neon gaseous laser operating in the visible red region of the spectrum would be the ideal type to build for this project because power requirements would be small, and the continuous action and visibility of the red laser light would facilitate experimentation. It was decided to undertake the construction of

the lasers in order to maintain a maximum amount of flexibility within the system. This, then, is a report on the construction of a system; both the component laser design and the heterodyning techniques are discussed in detail.

1.2 Contents

Chapter II contains several laser homodyne methods for measuring electron densities in a plasma. They have been extensively treated in the literature and are presented here for completeness. The main emphasis of the chapter concerns a description of optical heterodyning techniques used to probe a plasma. Included also in this chapter are calculations to show the expected magnitude of the frequency shifts involved.

Chapter III presents information on several aspects of laser theory necessary to the understanding of optical heterodyning. Also presented here is an analysis of experimental data concerning the optimum design of helium-neon gaseous lasers. Unfortunately, it was not possible to treat general maser and laser theory in detail, so a previous knowledge of the subject on the part of the reader must be assumed. Several books on lasers which the author has found useful are listed in the bibliography.

Concerning Chapter IV, a great deal of information has been written on the theoretical aspects of both general

laser theory and the theory of operation of a helium-neon laser. However, a thorough search of the literature revealed that no detailed information on the actual construction of a gaseous laser existed. Such details as, for instance, the techniques of aligning the mirrors of the laser cavity would have saved many hours of time had they been known beforehand. This chapter was written with the hope of eliminating this gap between theory and practice.

Chapter V treats of the details of the beating experiments, including the methods of obtaining beat frequencies, and contains comments on various causes of instabilities in the system. Also presented here are proposals to reduce the instabilities or their deleterious effects.

Chapter VI deals with the conclusions formed from the work and recommends some topics for future study.

CHAPTER II

MEASUREMENT OF ELECTRON DENSITIES OF A PLASMA WITH A LASER SYSTEM

2.1 Introduction

At the present time several methods exist for measuring plasma electron densities as low as 10^{10} to 10^{12} particles/cc. These methods utilize either microwave or Langmuir probe techniques to obtain data on the electron density. In the former case the spatial resolution is quite limited due to diffraction effects. The best resolution for easily obtainable microwave apparatus capable of detecting small phase shifts is of the order of the microwave wave length (about 4 mm). It is often necessary to have a higher precision on spatial data. Langmuir probes can provide this precision but at least two objections can be raised regarding their use: (1) the possibility of the probe perturbing the plasma, and (2) the accuracy of probes when magnetic fields are present.

In this section a method will be presented for measuring electron densities over a wide range of values. Its advantages are that it does not perturb the plasma, has good time response, and provides excellent spatial resolution. Basically, it is an extension of microwave methods into the optical domain and consists of extremely precise determinations

of the index of refraction of the plasma. Two methods are available for making these measurements: (1) optical homodyning, in which phase changes are measured, and (2) optical heterodyning, in which the shift in the resonant frequency of the laser cavity is measured.

2.1 Optical Homodyning

The optical homodyning technique is shown in Fig. 2.1. It is an obvious extension of interferometry to laser technology. The phase detection is accomplished by comparing the phases of two beams which are formed by the primary beam splitter. The plasma tube is placed in one arm of the interferometer, and a laser is used as the light source.

The principle of operation is that for each half wave length change in optical path length B with reference to path A, the intensity of the light on the detector will change from zero to a maximum and back to zero again. This is a result of first, total destructive interference between beams A and B, then a constructive interference as the path length is increased by a quarter wave length, followed again by complete cancellation of the two beams a quarter wave length further along. The change in path length in this case is achieved through a change in refractive index within the plasma tube due to the electron density of the ionized gas. Quantitatively, the relative change in

Optical homodyning method for measuring plasma electron densities

Figure 2.1

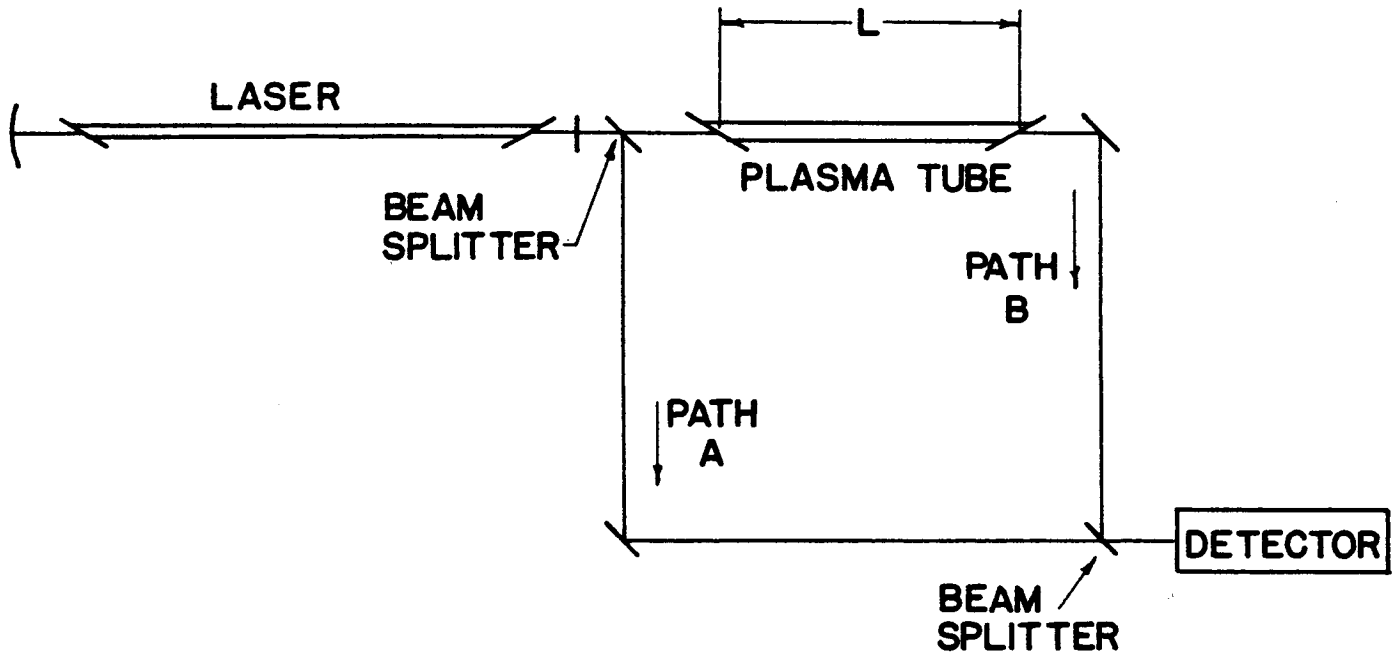
L
LASER
PLASMA TUBE
BEAM
SPLITTER
PATH
B
PATH
A
DETECTOR
BEAM
SPLITTER

length ($\Delta\phi$) between the two paths A and B of the interferometer is just equal to the change in the equivalent optical length, Ln, of the discharge tube, or

$$\Delta\phi = Ln - Ln', \tag{1}$$

where n and n' represent, respectively, the refractive index of the gas within the plasma tube and the plasma. It can be shown that n' is related to the plasma frequency, ν_p, by [1]

$$n'^2 = 1 - \nu_p^2/\nu^2, \tag{2}$$

or for $\omega_p << \omega$,

$$n' \simeq 1 - \frac{1}{2}\frac{\nu_p^2}{\nu^2}. \tag{3}$$

Inserting this equivalent relation for the plasma refractive index into equation (1) and approximating n by 1 gives

$$\Delta\phi = L/2\ \nu_p^2/\nu^2 = \frac{1}{2}L\ \nu_p^2\lambda^2/c^2, \tag{4}$$

where λ is the free space wave length of the laser output and c is the velocity of light. Now the plasma frequency may be expressed in terms of the electron density (N_e) by [1]

$$\nu_p^2 = 8.1 \times 10^7 N_e \text{ electrons/cc}. \tag{5}$$

Putting this relation into equation (4) gives the result

$$\Delta\phi = 4.5 \times 10^{-14}\lambda^2 N_e L, \qquad (6)$$

or in terms of the number of fringe shifts, q,

$$q = 9 \times 10^{-14}\lambda N_e L. \qquad (7)$$

For a helium-neon laser operating in the visible red at a wave length of 6328 Å and with a plasma column 1m long, it is found that a density of 5.6×10^{14} electrons/cc is necessary to produce one fringe, or a half wave length shift in path B. Thus, although fractions of a fringe may be measured photographically, the system basically has relatively poor sensitivity.

Another device operating on a similar principle is shown in Fig. 2.2.[2,3] It is found that when the laser beam is directed back through the laser tube by mirror A, the reflected beam interacts with the incident beam resulting in constructive or destructive interference at the detector.[4] The phase of the reflected beam, which determines the amount of interference, is dependent on the light path length between mirrors A and B, and either changing the position of mirror A or varying the refractive index of the material between the mirrors will affect the light intensity at the detector. Calculations show the same phase

Alternate optical homodyning method for measuring plasma electron densities

Figure 2.2

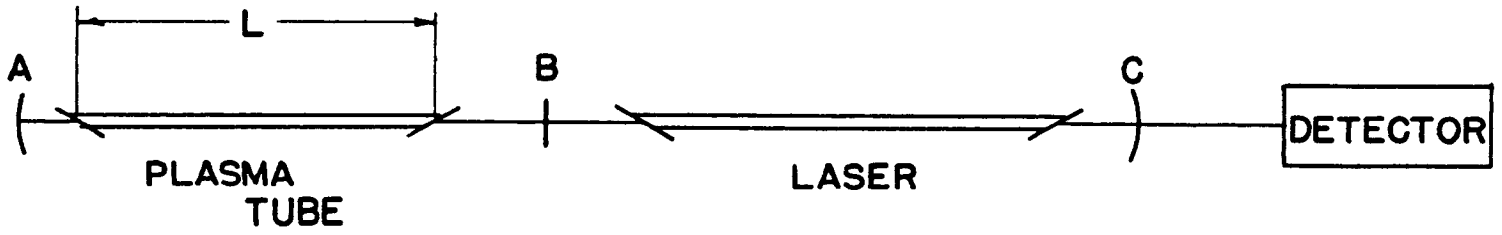
L
A
B
C
DETECTOR
PLASMA
TUBE
LASER

shifts will be obtained with this system as with the one described previously so that equation (7) is still applicable here.

2.3 Optical Heterodyning

An optical heterodyne system for the measurement of electron densities, originally proposed by Javan, [5] is shown schematically in Fig. 2.3. A discharge tube is inserted in the cavity with one of the lasers; the other laser serves as frequency reference or local oscillator in the system. The two outputs are positioned on the detector so that a resultant beat frequency between the two beams is observed. With both lasers operating and the plasma tube off, the beat frequency is noted on the spectrum analyzer. A plasma is now produced in the plasma tube; the effective index of refraction in the cavity is changed resulting in a different resonant frequency which gives rise to a new beat frequency. Knowing the frequency shift, the index of refraction and the electron density of the plasma may be calculated.

Let λ be the wave length of a laser with a cavity length ℓ and an index of refraction n; with no plasma in the cavity, the resonance condition may be approximated by*

$$\frac{1}{2} m\lambda = n\ell \qquad (8)$$

*See Chapter III, Section 3.6

where m is an integer of the order of 10^6. Placing a plasma column of length L in the cavity changes the above equation to

$$\frac{1}{2} m\lambda' = n(\ell-L) + n' L. \qquad (9)$$

Here, λ' is the new wave length due to a shift in frequency, and the other symbols are used above. Combining and rearranging equations (8) and (9) yields the relation

$$\frac{\Delta\lambda}{\lambda} = \frac{L}{\ell}\frac{\Delta n}{n}. \qquad (10)$$

Assuming that the value of the refractive index of air (n) is one, and using the value of the index of refraction of a plasma as given by equation (3), it is found that

$$\frac{\Delta\lambda}{\lambda} = \frac{1}{2}\frac{L}{\ell}\left(\frac{\nu_p}{\nu}\right)^2 \qquad (11)$$

Finally, recognizing the fact that $\Delta\lambda/\lambda = \Delta\nu/\nu$ and replacing ν_p by its equivalent in terms of electron density as given by equation (5), equation (11) becomes

$$\Delta\nu = 4.1 \times 10^7 \frac{L}{\ell}\frac{N_e}{\nu}; \qquad (12)$$

or, the change in frequency of the laser beam is inversely proportional to the frequency of operation, and directly proportional to the electron density and the ratio of plasma

column length to laser cavity length. Table 2.1 gives some values of frequency shifts for various electron densities at two presently practical values of the plasma column to cavity length ratio. For comparison, both the infrared 3.39 micron and the visible red .6328 micron laser oscillation wave lengths have been used in the calculation.

n_e	$\Delta\nu$			
	6328Å		3.39u	
	$L/\ell = 1/2$	$L/\ell = 1/10$	$L/\ell = 1/2$	$L/\ell = 1/10$
10^{10}	430 cps	86 cps	2300 cps	460 cps
10^{12}	43 Kcps	8.6 Kcps	230 Kcps	46 Kcps
10^{14}	4.3 Mcps	.860 Mcps	23 Mcps	4.6 Mcps

TABLE 2.1 - The effect of plasma electron density on laser frequency

2.4 Frequency Stability of a Heterodyne System

The beat frequency of a heterodyne laser system as described above is subject to a considerable amount of drift. It is easily shown, for instance, that the relationship between a change in cavity length and a change in frequency is given by $\Delta\nu/\nu = \Delta\ell/\ell$. For the 6328Å

Optical heterodyne system for determination of plasma electron densities

Figure 2.3

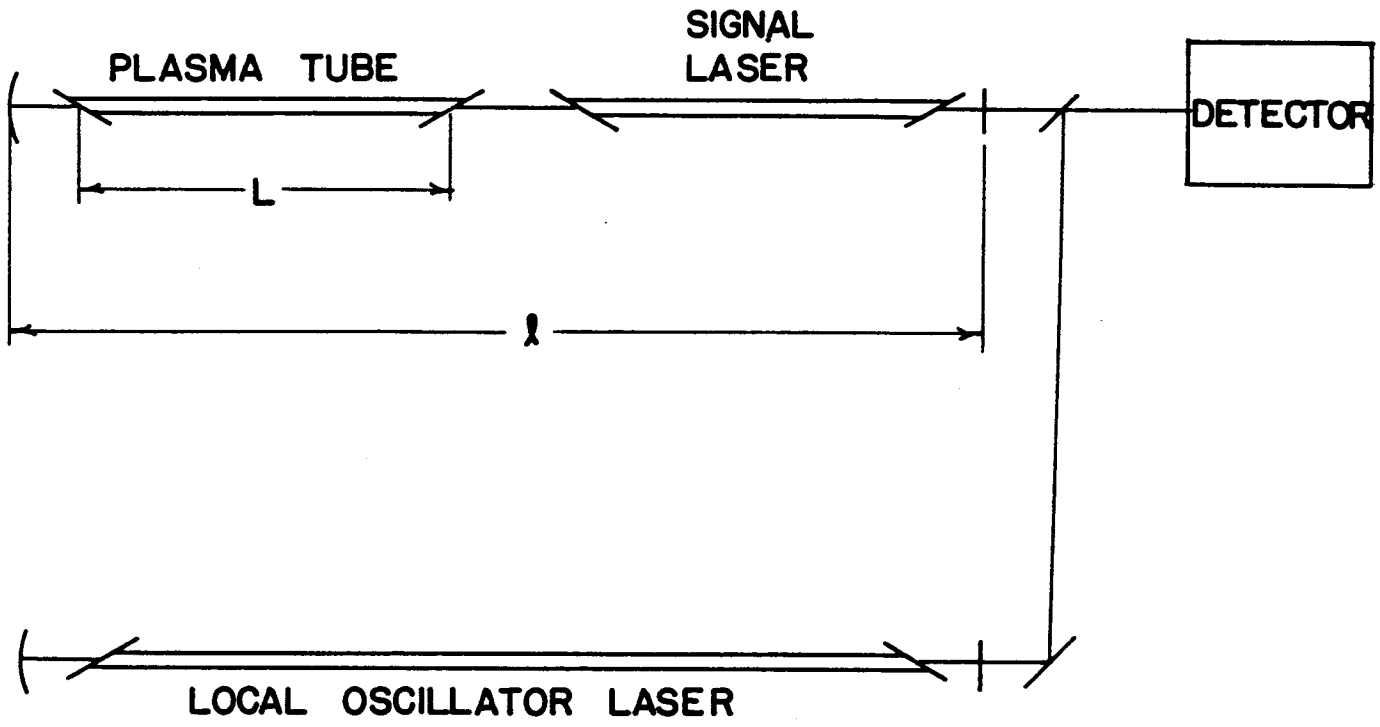
SIGNAL
LASER
PLASMA TUBE
DETECTOR
L
l
LOCAL OSCILLATOR LASER

visible red laser, a change in output frequency of 1 Mc/s is equivalent to a change in length of a one meter cavity of only 21Å. Obviously, then, from a practical standpoint the stability may be influenced by all manner of vibrations-acoustic, building, and thermal-to name a few. The former two may be substantially reduced by special shock mounting procedures. One such method is to install the laser table on a platform connected to the bedrock of the earth in an area isolated from heavy vehicular traffic and other sources of vibration. The thermal effects may be divided into an irreducible component due to thermal motion of atoms in the material separating the mirrors and a component due to temperature fluctuations. The former has been examined theoretically by Javan, et al.[6] It is concluded that for two mirrors separated by a material of uniform cross section, the fluctuation in frequency ($\Delta\nu_t$) is given as

$$\Delta\nu_t = \nu \left(\frac{2kT}{YV}\right)^{\frac{1}{2}} \tag{13}$$

where k is Boltzman's constant, T is the temperature, Y is Young's modulus, and V is the volume of the material separating the mirrors. If this material is a slab of cast iron 20 cm wide, 5 cm thick, and 100 cm long, the calculated frequency instability is about 1 c/s. This

represents the upper limit to the stability which can actually be achieved by a practical system. The drift in laser frequency ($\Delta\nu_T$) due to a change in temperature may be calculated by combining the resonant condition for a laser cavity given by equation (8) with the equation for the expansion of a body (ΔL) given by

$$\Delta L = L_T \frac{\alpha \Delta T}{(1 + \alpha T)}, \tag{14}$$

where L_T is the length of the body at temperature T in °C, and α is the coefficient of linear expansion. It is easily shown that the result may be approximated by

$$\Delta\nu_T = \alpha \nu \Delta T \tag{15}$$

Using the value of the coefficient of expansion for cast iron (the material from which the laser table is made), the change in frequency with temperature is found to be approximately 5 Mc/s/.001 °C. It must be remembered, however, that the tables on which a laser will usually rest are quite massive and as a result are not very amenable to large temperature changes over short periods of time. Temperature changes, from the very nature of their effect, are not likely to be important in producing short term frequency fluctuations, but they are probably very important from the standpoint of long term stability.

Javan, et al. [6,7] have, after considerable effort,

succeeded in closely approaching the limits of stability. They have obtained short term frequency fluctuations in a helium-neon laser of the order of 30 c/s over a period of several seconds. The long term stability achieved was of the order of 6 Kc/s over a period of two minutes.

2.5 Detection of the Heterodyne Signal

The heterodyning of the outputs of two lasers is possible because of two unique characteristics of laser light, its time and space coherence. Time coherence means that as a wave front passes through space, the field intensity at a stationary point will vary sinusoidally with time. Spatial coherence is a correlation between the phases of monochromatic radiation arising from different points of the radiator. Thus, waves from two different sources are able to interact in such a manner as to cancel or reinforce one another at the photosensitive surface of a detector.

The beat signal between the optical frequencies is detected by positioning the accurately superimposed outputs of the two lasers on the sensitive surface of a phototube. The total output power of the phototube is directly proportional to the intensity of the light incident upon it, but the intensity is proportional to the square of the total electric field of the incident

radiation. Moreover, the total electric field (E_T) is composed of the electric fields of the signal laser (E_s) and the local oscillator laser (E_o) (the laser outputs are assumed plane polarized) operating at frequencies ω_s and ω_o respectively. Therefore, the total phototube input power (P_T) is given as

$$P_T \alpha \underline{E}_T^2 = (\underline{E}_s + \underline{E}_o)^2 \, . \tag{16}$$

Expanding the above equation further gives

$$\begin{aligned}(\underline{E}_s + \underline{E}_o)^2 &= (E_s \cos \omega_s t + E_o \cos \omega_o t)^2 \\ &= E_s^2 \cos^2 \omega_s t + E_o^2 \cos^2 \omega_o t \\ &\quad + 2E_s E_o \cos \omega_s t \cos \omega_o t,\end{aligned} \tag{17}$$

or by using common trigonometric identities, one obtains

$$\begin{aligned}(\underline{E}_s + \underline{E}_o)^2 &= E_s^2 (\tfrac{1}{2} + \tfrac{1}{2} \cos 2 \omega_s t) \\ &\quad + E_o^2 (\tfrac{1}{2} + \tfrac{1}{2} \cos 2\omega_o t) \\ &\quad + E_s E_o \cos (\omega_s - \omega_o) t \\ &\quad + E_s E_o \cos (\omega_s + \omega_o) t\end{aligned} \tag{18}$$

Therefore, assuming that the sum and double frequency com-

ponents may be neglected, the total power input to the phototube has both alternating and direct current components given by

$$P_T = P_{ac} + P_{dc} \tag{19}$$

$$\alpha\ E_s E_o \cos(\omega_s - \omega_o)t$$

$$+ \frac{1}{2}(E_s^2 + E_o^2)$$

or in terms of the signal and local oscillator amplitudes, A_s and A_o

$$P_T = A_s A_o \cos(\omega_s - \omega_o)t$$

$$+ \frac{1}{2}(A_s^2 + A_o^2)\ . \tag{20}$$

2.6 The Signal-To-Noise Performance of a Heterodyne System

For the purpose of this discussion the dark current and the effects of background radiation will be considered as negligible sources of noise in the phototube; also, it will be assumed that thermal noise can be neglected. Thus, the shot noise is the dominant source of noise in the system. The current i which is generated by the phototube is given by the relation [8]

$$i = \eta e P/h\nu\ , \tag{21}$$

where η is the quantum efficiency, e is the magnitude of the electron charge, P is the input power to the phototube, and $h\nu$ is the quantum energy. The signal power is given by the ac component of the input power as determined by equation (20), so the signal photo current, i_s, is

$$i_s = \frac{ne}{h\nu} A_s A_o \cos(\omega_s - \omega_o)t \qquad (22)$$

which has a mean square value of

$$\overline{i_s^2} = \frac{1}{2}\left[\frac{ne}{h\nu} A_s A_o\right]^2 \qquad (23)$$

The mean square value of the shot noise current is given by

$$\overline{i_n^2} = 2\, e\, B\, i_{dc} \qquad (24)$$

where B is the bandwidth of the circuitry following the phototube. By using equation (21) for the photo current in terms of the power, and the dc component of the power from equation (20), the noise current is found to be

$$\overline{i_n^2} = \frac{ne^2}{h\nu} B\,(A_s^2 + A_o^2)\,. \qquad (25)$$

The signal-to-noise ratio is determined by the ratio of the signal output power to the shot noise power, or equivalently, the ratio of the mean square signal current to

the mean square noise current; thus

$$\frac{S}{N} = \overline{i_s^2} \,/\, \overline{i_n^2}$$

$$= \frac{\eta}{2h\nu B} \frac{A_o^2 \quad A_s^2}{A_o^2 + A_s^2} \tag{26}$$

It is easily determined that the signal-to-noise ratio is maximum for very strong local oscillator power. Then, for a large value of A_o^2 the signal-to-noise ratio becomes

$$\frac{S}{N} = \frac{\eta}{h\nu B} \frac{A_s^2}{2}$$

$$= \frac{\eta \overline{P}_s}{h\nu B} \tag{27}$$

where $\overline{P}_s$ represents the average value of the signal power.

2.7 The Nonlinear Frequency Response of a Laser

One shortcoming in the apparent value of the proposed electron density measurement scheme is that the shift in laser output frequency ν_o is not equivalent to, or even simply related to, the cavity frequency ν_c, although for most purposes it is a very good approximation. The full width at half maximum of the cavity frequency of oscillation, $\Delta\nu_c$, is much more narrow than the corresponding width of the Doppler broadened radiative laser transition, $\Delta\nu_D$. As a result, several longitudinal modes of oscillation

(these are represented by unit changes of the value of m in equation (8); i.e., m-2, m-1, m, m+1, m+....) may exist simultaneously in a laser cavity with each mode being free to roam over a limited region of the Doppler broadened transition in the event of a change of cavity resonant frequency. It is found, moreover, (and this is the drawback in the scheme) that the frequency separation between adjacent longitudinal modes becomes smaller as their distance from the peak of the Doppler broadened transition, ν_D, is increased. Thus, in effect the oscillating modes are attracted toward ν_D with an intensity that is proportional to their distance from it.

Unfortunately this mode pulling, as it is commonly called, is not simply related to the distance from the center of the transition but is a function of mainly three phenomena: [10, 11] (1) a frequency pulling due to the difference in resonant frequency between the cavity and atomic laser transition, (2) a change of refractive index of the amplifying medium as the distance from ν_D is increased, and (3) an effect called hole repulsion. The first of these is very similar to an effect encountered in an electronic crystal controlled oscillators. If the tank circuit of such a device is slightly detuned from the resonant frequency of the crystal, oscillation will occur somewhere between the two at a frequency dependent on the

relative Q of each component oscillator. Similarly, in the case of the laser, the two mirrors are effectively the equivalent of one oscillator and the atomic upper and lower laser levels, the other. The expression for the actual frequency of oscillation, ν_o, is given by

$$\nu_o = \frac{\nu_D \Delta\nu_c + \nu_c \Delta\nu_D}{\Delta\nu_D + \Delta\nu_c} \tag{28}$$

Quantitatively this amounts to a frequency separation between axial modes of about 100 Kc/s less than the commonly used 150 Mc/s (given by $c/2\ell$) for a visible red helium-neon laser with a 1m cavity. Referring to the second phenomenon, it has been found [11] that the index of refraction within a laser tube is an intricate non-linear function of both the frequency of the amplifying transition and the number of atoms contributing to laser action. The ultimate consequence of this is that cavity resonances below the peak, ν_D, of the amplifying transition have their frequency raised. The third effect, hole burning, is caused by a depletion of excited atoms at a particular cavity resonant frequency within the broad amplifying transition. This is possible because different atoms contribute to the gain over various sections of the line, a consequence of the collision frequency being smaller

than the spontaneous decay rate of the upper laser level. The result may be pictured as a Doppler broadened gain curve with dips or holes in it at the frequencies of laser oscillation. These holes tend to repel each other causing an increase in the beat frequency between adjacent longitudinal modes.

The question arises then, with all of the non-linear effects acting on the output frequency of a laser, how is it possible to relate the observed change in frequency to the actual change in index of refraction within the plasma tube, or equivalently, to relate the change in frequency with the change in length of the laser cavity? It has been observed by Bennett [10] that the dominant mode pulling mechanism in a laser is that given by equation (15) above. If this is used as the single source of error in a heterodyne system, a correction factor can be calculated in the following fashion: Consider a system using a visible red helium-neon laser with a one meter cavity. For the condition $\Delta\nu_c << \Delta\nu_D$, equation (15) can be shown to give a frequency separation between adjacent longitudinal modes of

$$(\nu_o' - \nu_o) \simeq (\nu_c' - \nu_c) \quad (1 - \frac{\Delta\nu_c}{\Delta\nu_D}). \tag{29}$$

where the primed quantity represents the mode adjacent to

the unprimed quantity. This actually is equivalent to the shift in frequency one mode will undergo if the cavity length is increased by an amount equal to $m\lambda/2$ (equation 8). The amount of correction necessary per observed megacycle shift in frequency is given as

$$\underset{\text{(cps/megacycle)}}{\text{correction factor}} = \frac{(\nu_o' - \nu_o) - (\nu_c' - \nu_c)}{(\nu_o' - \nu_o)} \qquad (30)$$

and is approximately equal to $\Delta\nu_c/\Delta\nu_D$ for $\Delta\nu_c \ll \Delta\nu_D$. For the present case $\Delta\nu_c$ is one megacycle per second and $\Delta\nu_D$ is one and a half gigacycles per second, giving a correction factor of 666 c/s per megacycle change in frequency as indicated by the detector. For the case of the 3.39 m laser transition, the correction is approximately 4 Kc/s per megacycle change in frequency.

CHAPTER III

THEORY OF OPERATION OF A HELIUM-NEON LASER

3.1 Introduction

In its most elementary form, a laser consists of an amplifying medium situated between two mirrors which form a Fabry-Perot interferometer. A wave front passing through the medium increases in intensity by stimulating properly excited atoms to emit energy. Upon reaching the mirror, part of the light beam is absorbed, some transmitted, and part is reflected back into the amplifying medium to gain more intensity. If the intensity gain per pass between the mirrors of the interferometer is greater than the various losses, oscillation will take place and the system is said to "lase". A significant aspect of the stimulated wave is that its phase coincides exactly with that of the stimulating wave front. This leads to one of the most important properties of laser light, namely, its space and time coherence, the other being its high intensity.

Laser action was first obtained in the visible region in a solid state device using a ruby crystal as the amplifying medium. Shortly thereafter, laser action was observed in the infrared in a gaseous device utilizing a mixture of helium and neon. Eventually this device was also found to

lase in the visible region at a wave length of 6328Å. Many new laser materials have been discovered and many new laser transitions observed since these first two were originally developed. For the purposes of this thesis, however, it was decided that the most practical device to investigate was a continuous-wave helium-neon laser operating in the red region of the visible spectrum.

3.2 Light Amplification

The phenomena of laser action is completely dependent on the ability of a wave front passing through an amplifying medium to induce properly excited atoms to give up their energy to it. The criterion for this stimulated emission to take place is just that the energy between two excited states, or between an excited state and the ground state, of an atom be equal to Plank's constant, h, times the frequency, ν, of the passing wave front, or

$$E_2 - E_1 = \Delta E = h\nu \qquad (1)$$

where E_2 and E_1 represent respectively the upper and lower energy states of the atom.

Einstein first postulated the existence of induced emission and was able to show that the probabilities of absorption and stimulated emission were proportional. It can be shown that generally for equilibrium conditions more atoms will be excited in the lower rather than the

upper energy state. Under these circumstances the amplitude of a plane wave passing through a medium will decrease because more atoms will absorb than emit energy. In order to amplify the wave front then, a population inversion (i.e., the number of atoms in energy state E_2 is greater than that in E_1) must be formed in some manner. In the helium-neon laser operating in the visible this is accomplished mainly through two mechanisms: [12, 13] excitation of the long-lived neon $3s_2$ upper laser level by resonance collision with metastable 2^1S helium atoms, and a swift depopulation of the $2p_4$ lower laser level by fast transitions to lower energy states. Fig. 3.1 illustrates the described energy level diagram for the helium-neon laser.

3.3 Limits on Laser Tube Diameter and Gas Pressure

From a practical standpoint, the gas is held within the cavity by a glass tube and excited by either radio frequency energy or a direct current discharge. A limit exists on the maximum diameter of the tube, however, for it has been experimentally determined that the gain is approximately inversely proportional to the tube radius. The maximum diameter of a helium-neon laser tube is probably in the vicinity of 2.5cm. The most commonly encountered diameters in present day work range from 1 to 6 mm.

Energy level diagram for the helium-neon laser

Figure 3.1

ENERGY LEVEL DIAGRAM FOR THE HELIUM-NEON LASER

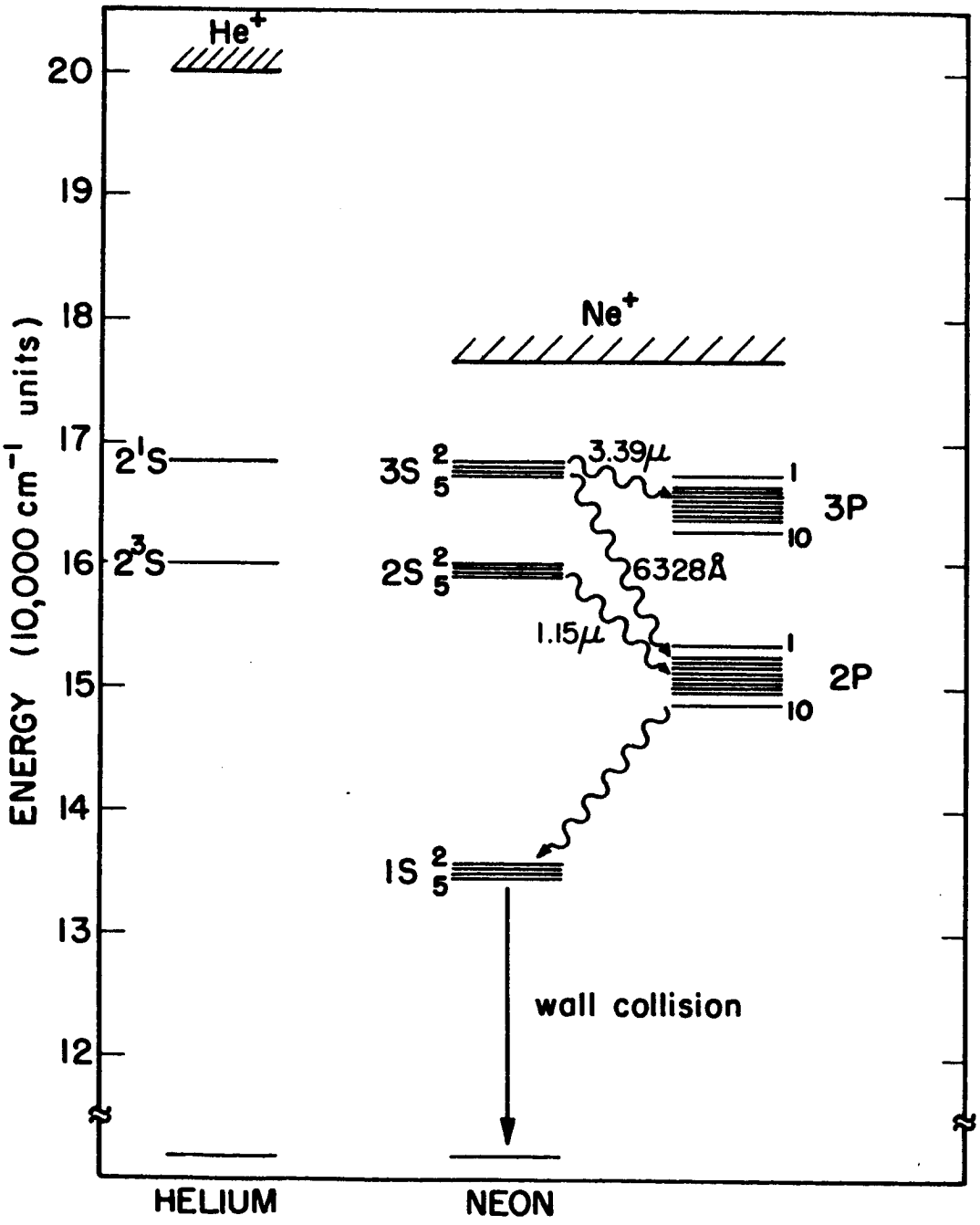

Gordon and White give an empirical relation between the tube pressure, p, and the diameter, d, as

$$p\,d = 2.9 - 3.6 \quad \text{Torr-mm} \qquad (2)$$

with the low figure appropriate for small diameter tubes. The results obtained in this laboratory differ somewhat. Some possible reasons for the discrepancy are a difference in the physical construction of the laser tube, a different method of exciting the gas, or impurities in the commercially obtained helium-neon gas mixture used.* Fig. 3.2 shows a graph of relative laser power output vs input current with pressure as a parameter. The ratio of the helium-to-neon pressure was seven to one. The tube diameter was approximately 2.8 mm and the active discharge length was 37 cm.

3.4 Effects of Gas Pressure and Tube Current on Laser Power

Before attempting to analyze the variation of laser output power with gas pressure and tube current, several observations can be made regarding the various mechanisms affecting population inversions in a mixture of helium and neon gas. In summary, Gordon and White [13, 14] have shown:

*The helium-neon gas was purchased from the Linde Co., Division of Union Carbide Co., Tonawanda, New York.

Relative laser output power vs. tube current

Figure 3.2

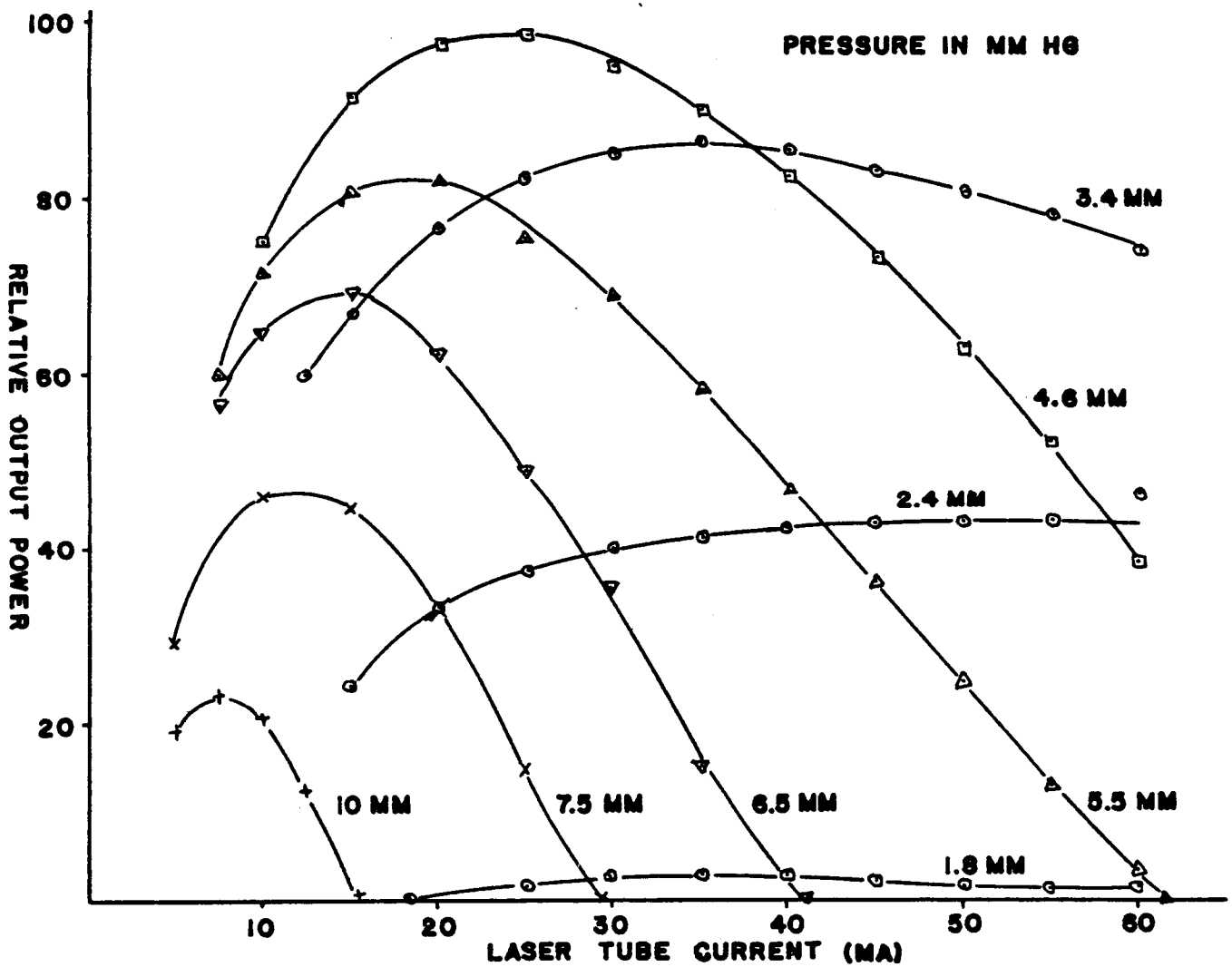
PRESSURE IN MM HG
3.4 MM
4.6 MM
2.4 MM
10 MM
7.5 MM
6.5 MM
5.5 MM
1.8 MM
RELATIVE OUTPUT POWER
100
80
60
40
20
10
20
30
40
50
60
LASER TUBE CURRENT (MA)

1. The average electron density is proportional to the discharge current.
2. The average electron energy is independent of the discharge current.
3. The neon $3s_2$ upper laser level is predominantly excited by resonance collision with the helium metastable 2^1S level.
4. The population density of the helium 2^1S level exhibits a linear increase with current for small currents but saturates at high currents, indicating that at high electron densities (order of 10^{11}/cc) electron collisions become a dominant loss mechanism.
5. The decrease in population of the upper laser level by radiation to the ground state is a function only of gas pressure and laser tube diameter.
6. The lower laser level is populated mostly by radiative transitions from higher levels and direct electron impact with the ground state atoms (the former mechanism is proportional to the electron density and the gas pressure).
7. The radiation loss of the lower laser level is independent of pressure.

Referring to Fig. 3.2, it is seen that as the pressure is increased to about 3mm Hg in the laser tube with the dis-

charge current below 40 ma, power output increases owing to an increase in the population of the neon $3s_2$ upper laser level. As the current is increased beyond 40 ma, the lower laser level becomes more densely populated due to an increase in radiative transitions from upper states (as a result of an increase in excitation rate) and electron collisions with ground state neon atoms; thus, laser power decreases. As the pressure is increased beyond 3mm Hg, the output power begins to fall off quite rapidly at tube currents in excess of 30 ma; it is likely due to the increasing effectiveness of electron collisions in populating the lower laser level, although the pressure sensitive radiative transitions from upper energy levels are also an important contributing factor. The point of peak output power is seen to move in the direction of lower currents as higher gas pressures are attained in the tube; the shift is a result of the slight dependence on pressure of the upper laser level population density. Beyond 5mm Hg pressure, radiative transitions from the upper laser level to the ground state become increasingly important in upsetting the population inversion necessary for laser action. This is shown by the rapid decrease in peak putput power with increasing pressure.

3.5 The Fabry-Perot Cavity

The Fabry-Perot interferometer is a multimode resonant

cavity which supplies the positive feedback necessary to produce laser oscillation with a helium-neon gas discharge. It is composed of two mirrors, the surfaces of which are accurately finished to within a fraction of a wavelength of light and coated with a multilayer dielectric film for maximum reflectivity and minimum absorption loss. Reflection coefficients of 99.5% are not uncommon and are actually necessary to provide the high gain necessary for laser action in a visible red helium-neon laser.

Cavities can be classified according to the type of mirrors used into three main categories: the plane parallel, the spherical, and the hemispherical. The plane parallel cavity utilizes two flat mirrors and is the type Javan, et al. [15] employed in the original gas laser. This configuration is not very often used, however, because of the extremely critical tolerances (about ±3 seconds of arc) on the angular adjustment of the mirrors necessary to allow the tube to lase. The second type of cavity utilizes two spherical mirrors and can be further subdivided into two divisions. The first is the confocal cavity which operates with a mirror separation equal to the radius of curvature of the mirrors; it represents the lowest loss cavity available. The second is the concentric cavity with a mirror separation equal to twice their radius of curvature. An interferometer employing

spherical mirrors is not necessarily restricted to operate with the above two separations, however.[16] Typical alignment tolerances on spherical mirrors are of the order of three minutes of arc for the confocal and less than ten seconds for the concentric configuration. The third type, intermediate between the spherical and plane parallel, is the hemispherical cavity, utilizing one flat and one spherical mirror. The alignment tolerances lie somewhere between that of the plane parallel and confocal types, depending upon the placement of the laser tube within the cavity and the separation of the mirrors. It has the advantage of giving a less divergent beam than that commonly found with the spherical cavities while retaining the ease of alignment.

3.6 Cavity Modes

Boyd and Kogelnik [17] have considered theoretically and Goldsborough [18] has verified experimentally, the frequency characteristics of a laser cavity consisting of two spherical mirrors. The resonant frequencies, ν_c, of such a cavity are given by the expression

$$\nu_c = c/2d\,[m + (1 + p + q)f] \qquad (3)$$

where

$$f = \pi^{-1} \cos^{-1} [(1-d/b_1)\,(1-d/b_2)]^{1/2} \qquad (4)$$

and b_1 and b_2 are the radii of curvature of the mirrors separated by a distance d. The longitudinal mode number, m, is equal to the number of half wave lengths in the distance d and is of the order of 10^6 for a one meter mirror separation. The transverse mode numbers p and q can have any integral value. For the purpose of this paper a laser will be operated in a single transverse mode set (i.e., a particular value of p and q) which will not change with mirror separation. Since the quantity

$$f(1 + p + q) /m << 1 \tag{5}$$

for all cases of interest, the cavity frequency may be approximated by

$$\nu_c = \frac{c}{2d} m \tag{6}$$

It is interesting to note that a helium-neon laser ordinarily operates in several longitudinal modes simultaneously. The frequency separation between adjacent longitudinal modes is determined by c/2d and is about 150 megacycles per second for a one meter cavity. The radiative laser transition is Doppler broadened, the full width at half power being given by

$$\Delta\nu_D = 2\nu_o \sqrt{2kT/Mc^2 \ln 2} \approx 1500 \text{ Mcps} \tag{7}$$

where k is Boltzmann's constant, T the absolute temperature, and M the mass of the atom. Thus, for a helium-neon laser operating in the red region well beyond threshold power (the point where it just begins to lase), theoretically as many as ten longitudinal modes may be excited simultaneously. In practice the gain is sufficient to support only three or four modes.

3.7 The Brewster's Angle Windows

The mirrors on the first gaseous laser of Javan [15] were an integral part of the discharge tube and were attached to the ends of it with bellows to allow for the precise adjustments necessary to secure laser action. As a result of this cumbersome fabrication, the multilayer dielectric coatings of the mirrors came in contact with the discharge and were quite often destroyed by it. This construction also made it inconvenient to change the mirrors if it was necessary to operate the laser at a different frequency. Mirrors can be mounted externally if optically flat windows are sealed to the ends of the discharge tube. A theoretical analysis shows, moreover, that there is an angle of least loss at which to mount the windows. As indicated in Fig. 3.3, consider a beam of light, I_i, impinging on the surface of a material of refractive index n', at some angle θ; the transmitted beam,

Reflection and transmission of a beam of light

Figure 3.3

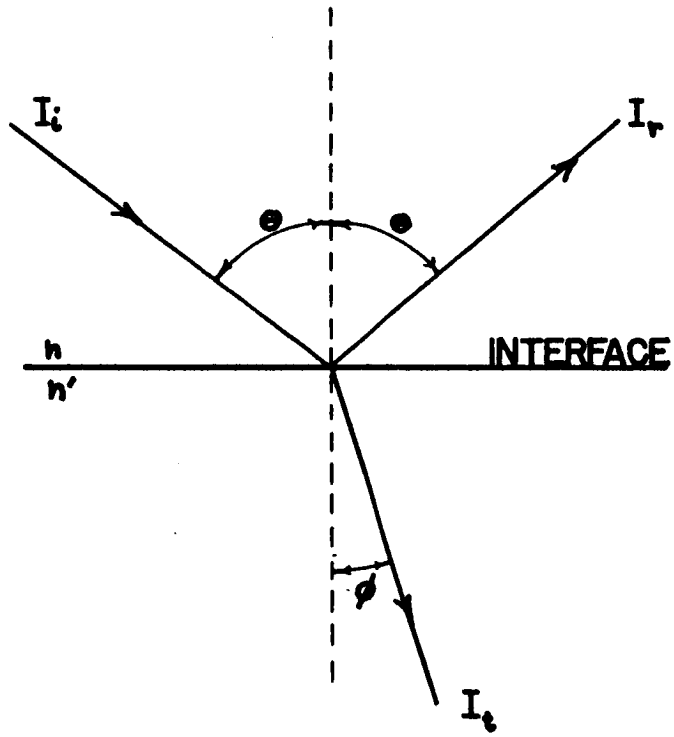
I_i
I_r
θ
θ
n
n'
INTERFACE
ϕ
I_t

I_t, forms an angle ϕ with the normal to the surface, while the angle of the reflected beam, I_r, is equal to that of the incident beam. As shown by electromagnetic theory, a light ray is composed of mutually perpendicular oscillating electric (E) and magnetic (H) fields. Since one field may always be specified in terms of the other (i.e., they are not independent), and since it is the square of the amplitude of E to which the intensity of light is proportional, it is convenient to eliminate the magnetic and use only the electric field vector. Now the electric vector of a ray of light interacting with a material may be broken up into a component perpendicular ($E_{i\perp}$) to the plane formed by the incident and reflected ray, and one parallel ($E_{i||}$) to it. The solution of Maxwell's equations for a plane wave moving through space, coupled with pertinent boundary conditions, will yield expressions for these parallel and perpendicular components of the electric field of the reflected ray as a function of the angles of incidence and refraction. For the parallel polarized component, it can be shown that

$$E_{r||} = E_{i||} \frac{\cos\theta - n/n' \cos\phi}{\cos\theta + n/n' \cos\phi} \qquad (8)$$

where the relation between the angles θ and ϕ is given by Snell's law;

$$n \sin\theta = n' \sin\phi. \tag{9}$$

Also, for polarization perpendicular to the plane,

$$E_{r\perp} = -E_{i\perp} \frac{\cos\phi - n/n' \cos\theta}{\cos\phi + n/n' \cos\theta}. \tag{10}$$

The gas atoms of the laser may be stimulated to emit light in a particular polarization; therefore, if the polarized reflection losses represented by either equation (8) or (10) can be made equal to zero for a particular angle, the theoretical transmission losses, at least, can be made equal to zero for that polarization. An examination of either the parallel or the perpendicular polarization cases with the plane wave normally incident on the glass ($\theta = \phi = 0$) discloses losses in both modes. Choosing a typical value for the index of refraction of glass as 1.5 and approximating the value of air as $n = 1$, it is found that the intensity of the reflected light is 4% of the incident light for either mode of polarization. Further examination of equation (10) shows that it can never be zero because $\theta > \phi$ by Snell's law (eq. 9).

Returning to equation (8), it is found that when $\sin \theta = \cos \phi$, that is, the reflected and refracted ray are mutually perpendicular, $E_{r||}$ is zero and all the parallel polarized light is transmitted. The angle θ, commonly expressed as $\theta = \tan^{-1} n'$, for which reflection losses are zero is known as Brewster's angle.

CHAPTER IV

THE DETAILS OF CONSTRUCTION OF LASERS

4.1 Introduction

This chapter contains detailed information on the construction of lasers. The physical structure of the laser tube is first considered. This is followed by a thorough treatment of the Brewster's angle windows (necessary with the use of external mirrors) of the tube. The procedure for preparing the tube for filling with helium-neon gas is presented, followed by an account of several methods of aligning the mirrors of the Fabry-Perot cavity. Finally, miscellaneous equipment such as mirror mounts, optical benches, the vacuum system, and so forth is described.

4.2 The Laser Tube

The essential features of the laser tube design are shown in Fig. 4.1. Pyrex glass rather than quartz was chosen for construction to reduce the loss of helium by diffusion. The glass tubing is heavy walled capillary with a nominal 2.5 to 3mm inside diameter and a 3/8 inch outside diameter. The sturdiness of the tube eliminates the need for a center support on the tube to prevent it from sagging; it also helps to prevent torquing around the tube axis which results in a misalignment of the

The laser tube

Figure 4.1

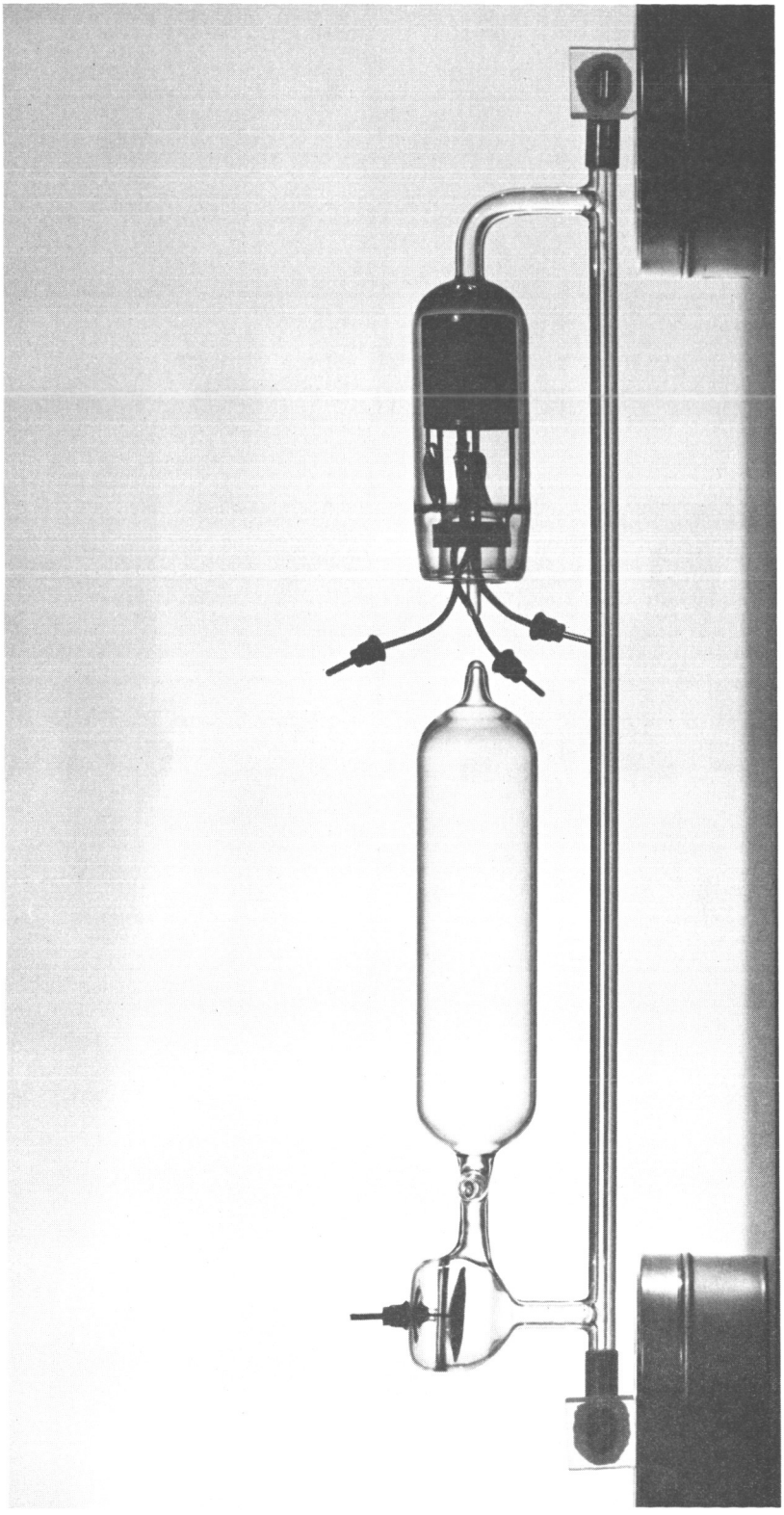

Brewster's angle windows. The electrodes are usually connected 1 1/2 inches from the ends of the tube. This prevents the deterioration of the epoxy resin, used to cement the metal sleeve to the tube, by the heat of the discharge. The glass bulb or ballast tube connected to the anode housing was added to compensate for the decrease in laser tube gas pressure which is apparently caused by the getter action of the electrodes.

4.3 Brewster's Angle Windows

During the early stages of this project it was thought that the tolerances on the window angles would be quite critical. As a result many fabrication problems were encountered because of the inability of existing facilities to cut glass accurately. A stainless steel sleeve, cut at the Brewster's angle and attached to the tube with epoxy resin, was finally used to circumvent the necessity of cutting the glass tubing. Later experimentation proved, however, that the angular tolerances were not severe. Using a laser with approximately a forty centimeter active discharge length in a hemispherical cavity, a window could be inserted in the beam within the cavity between about plus or minus twenty-five degrees without extinguishing laser action. It is also felt, on the basis of cursory observation,

that the tolerance on the skewness of the windows (i.e., the perpendiculars to the windows not lying in the same plane) is about three degrees.

The first type of windows* to be used on a laser tube were made of quartz with surfaces polished flat to 1/20 λ. Later several types of government surplus optical flats† were tested and found to make a completely satisfactory window. For the purposes of proposed experiments, no advantages have been found in the use of the quartz windows.

A recurring problem on early lasers was that the epoxy resin pulled away from the windows, allowing air to enter the tube and contaminate the discharge. This is a result of a difference in coefficient of expansion between the optically flat glass and the epoxy. The problem can be eliminated by sandblasting that portion of the window to come into contact with the epoxy resin. In order to protect the center portion of the window from the effects of the sandblasting, 1/16 inch thick sheet rubber can be attached to the glass with rubber cement.

* Brewster angle windows purchased from the Perkin-Elmer Corp., Norwalk, Conneticut, at $375 per pair.

† Optical flats purchased from Edmund Scientific Company, Barrington, New Jersey, at $.50 each.

The need for extreme cleanliness of the windows cannot be over-emphasized. To illustrate this fact, it has been found that ordinary dust and cigarette smoke in the air will settle on a freshly washed window and decrease output power by a factor of two in about two hours. One satisfactory cleaning method is the following: The windows are washed in a solution of distilled water and a household liquid detergent such as "Joy" or "Sail" followed by a rinse in distilled water. The windows are then rinsed with chemically pure acetone; finally, spectrograde acetone is poured over the surfaces and they are allowed to dry in the air.

4.4 Brewster's Angle Window Alignment

A schematic representation of the method of alignment of the Brewster's angles is shown in Fig. 4.2. A narrow, parallel beam of light is obtained using a lens and pin hole combination (a laser beam is an excellent substitute for the light source and lens), and the beam is reflected back upon the pin hole using the mirror. The laser tube is then positioned so that the light passes down the tube. Knowing the Brewster angle, θ, and the length of the tube, L, the angle ϕ, and hence the distance M to card C may be computed. A fraction of the light from the pinhole will be reflected from window

Method of aligning Brewster's angle windows using stainless steel sleeves

Figure 4.2

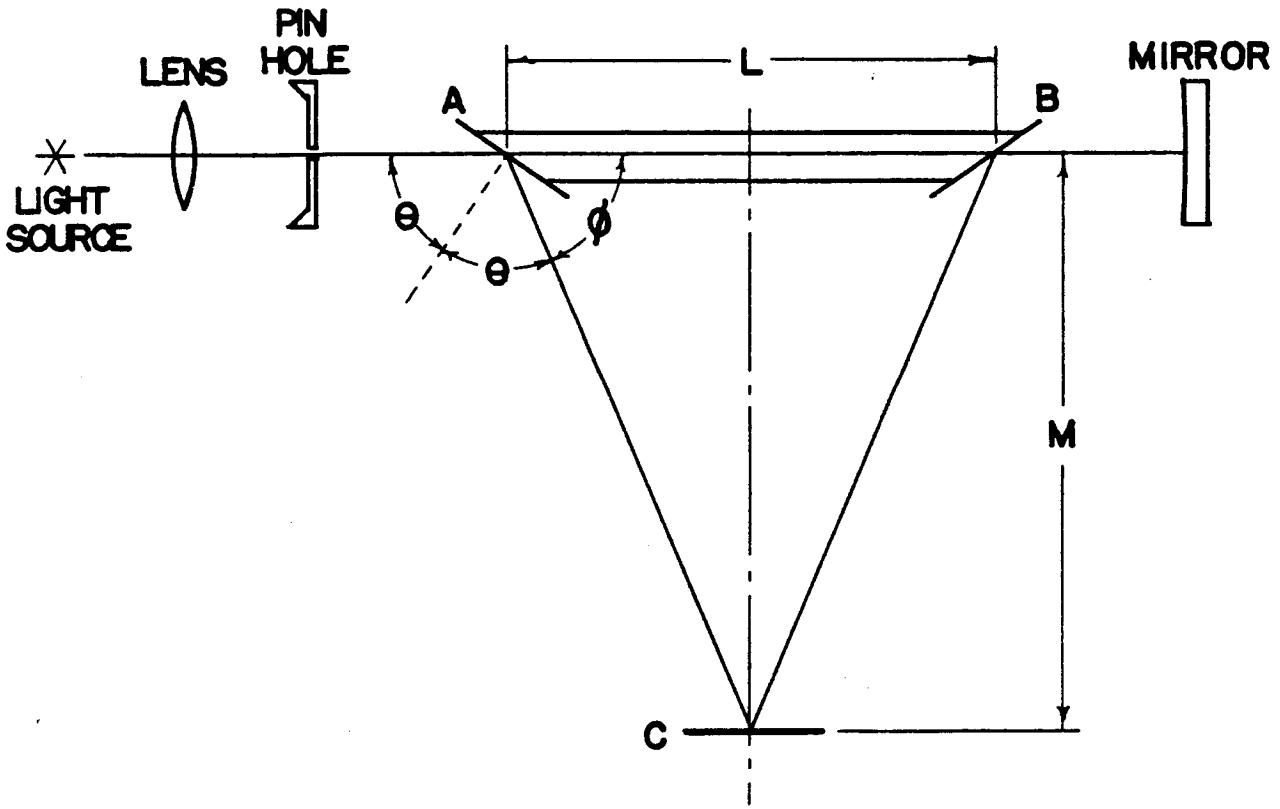
PIN
HOLE
LENS
L
MIRROR
A
B
LIGHT
SOURCE
θ
θ
ϕ
M
C

A onto card C, and part of the light returning from the mirror will be reflected by window B onto C. The diameter of the sleeves is slightly larger than the diameter of the glass tube, so the angle of the window may be altered alightly. The two reflected spots may thus be superimposed on card C serving to properly adjust the windows. The sleeves are then fastened to the tube with epoxy resin.

A method which would eliminate the need for the stainless steel sleeves has been proposed. Referring to Fig. 4.3, a length of tube with one end cut at approximately Brewster's angle is slipped over and joined to the laser tube. After the windows are cemented in place, the tube may be positioned in a contrivance as shown in Fig. 4.2. If heat is now applied to the glass at B until it just begins to soften, the angle may be accurately adjusted using the electrode port as a lever.

4.5 Electrodes

The electrodes* are parts of an unactivated 6011 mercury thyratron. The oxide-coated cathodes are rated at 2 1/2 amps average current, 30 amps maximum, with a filament current of 9 amps. Nonex glass is used in the construction of these parts, necessitating a cobalt seal

* Purchased from the General Electric Company, Tube Division, Owensboro, Kentucky.

Proposed glass joint to eliminate stainless steel sleeve

Figure 4.3

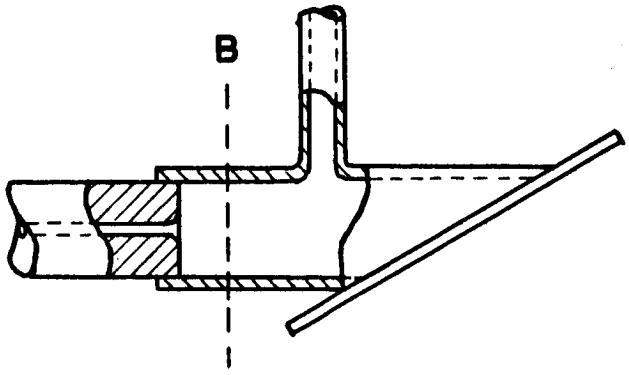
B

between them and the pyrex glass of the laser tube. At the present time, an entire laser tube is being constructed of Nonex glass to eliminate the need for the graded glass seal. One disadvantage of the cathodes is that on some tubes the oxide coating flakes off and coats the surface of the windows at the end of the tube. This, of course, substantially reduces, or sometimes completely destroys, laser action.

4.6 Cathode Activation and Filling of the Tube

The tube is sealed directly to the vacuum system and pumped down. When the pressure decreases below 10^{-6} mm Hg, activation of the cathode is begun as follows: Using a variac, the filament current is gradually increased from 0 to 9 amps in a period of about 3 minutes and allowed to flow for 30 minutes. The current is then raised to 12 amps for 5 minutes, followed by an increase to 15 amps for 2 minutes. Following this, the filament current is returned to 12 1/2 amps for 12 to 15 hours. The cathode actuation is now complete. The tube is continuously pumped during the entire process so that the pressure remains below 50 microns.

After the tube has been evacuated to 10^{-6} mm Hg, it is filled to a pressure of 3mm Hg with a helium-neon mixture. A discharge is run at a current of 60 ma. for

approximately fifteen minutes followed by a re-evacuation to 10^{-7} mm Hg pressure. This process eliminates the need for a bake-out procedure because of the clean-up nature of the discharge. The tube will usually lase on the second filling, though four or five fillings are recommended to remove all traces of impurities before the tube is finally cut off the vacuum system.

4.7 Alignment of the Fabry-Perot Cavity

Before being installed in the cavity, the mirrors should be washed with a solution of distilled water and mild liquid detergent such as "Joy", followed by a rinse in distilled water. Air drying of the surfaces is preferred to wiping since they are easily scratched.

The mirrors are aligned as is shown in Fig. 4.4. The laser tube is placed between the two mirrors, and a beam splitter or mirror is inserted at one end of the cavity. A lens is used to focus the image of a flashlight bulb filament onto mirror B. The lens and lamp are then positioned until the filament image may be seen through the tube at point C. With the eye at D, mirror B is rotated until the reflected image of the filament is found. The process is now reversed to align mirror E. It is sometimes difficult to position the mirrors accurately enough for the tube to lase immediately,

Method of aligning mirrors

Figure 4.4

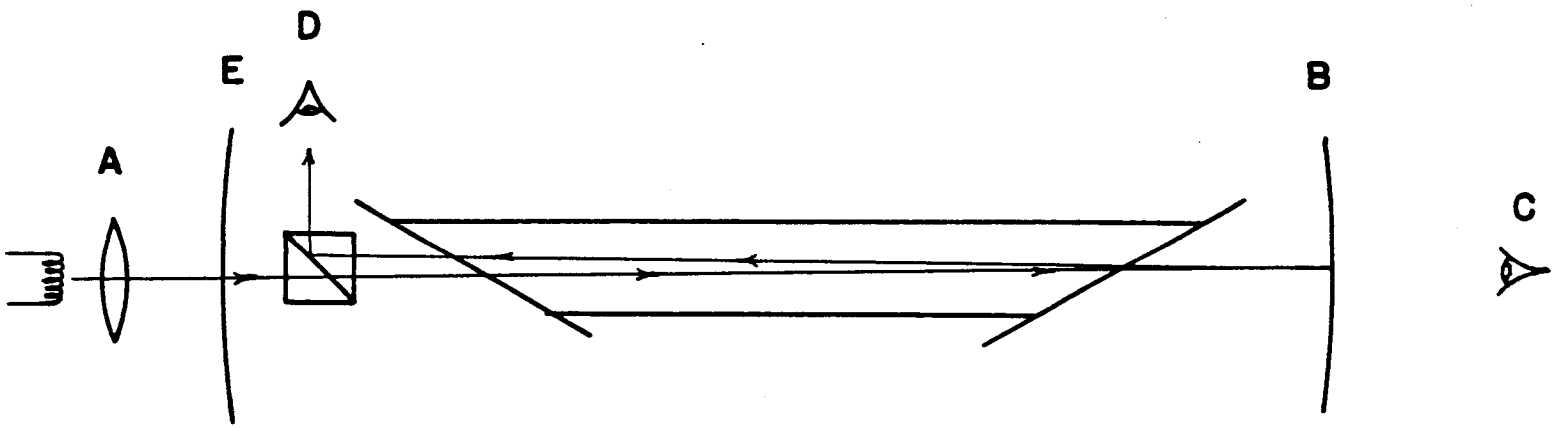
D
E
B
A
C

however, using this procedure, they are usually not misaligned by more than fifteen or twenty minutes of arc. Final adjustments necessary to obtain laser action can be made by sweeping through the region on either side of the setting of the adjustment knobs of one mirror mount.

Another scheme, more difficult to use but ultimately less time consuming and more accurate, is to use the laser tube to be aligned as the light source, hence eliminating the need for the lamp and lens in Fig. 4.4. A dense (3 Wratten ND 1.00 filters) neutral density filter must now be inserted between the beam splitter and the eye. By focusing the eye on the mirror at the end of the tube, one can see a reflected "moon" image. When the "moon" is centered in the tube, the mirror is aligned.

4.8 Vacuum and Gas Handling System

At the onset of this work, it was felt that a laser tube would suffer severely from any foreign gas that may have been left in the tube to contaminate the helium-neon gas mixture. Therefore a great deal of care was exercised in the selection of vacuum equipment and the construction of the system. The final system was built entirely of glass. It utilizes a Welch Duo-Seal Type

1402 fore pump with a cold trap and two Varian Associates 5 ℓ/s Vac-ion pumps. A Pirani gauge and a Granville-Phillips capacitive manometer are used to monitor the pressure. A Granville-Phillips Type C, Ultra-High Vacuum valve is used to isolate the fore pump and cold trap from the ultra high vacuum part of the system. Two other valves of this type are used to handle various helium-neon mixtures. With this system, pressures of the order of 10^{-8} mm Hg are very easily attainable in a reasonably short time. Once the cathode has been activated, a tube may be pumped down from 10 mm Hg pressure to 10^{-8} mm Hg in approximately 12 hours. It is interesting to note that the system has never been baked out. However, it was noticed that playing a Tesla coil over the surface of the glass tubing caused a temporary increase in pressure in the evacuated system after it had been exposed to atmospheric pressure; it is thought that the high voltage tends to dislodge air molecules adhering to the tube. This, rather than a bake-out procedure, was followed every time the system was brought up to atmospheric pressure.

4.9 Optical Benches

Two surplus machine shop layout tables were purchased to serve as optical benches. They are made from

cast iron, are 2 1/2' wide by 5' long, and weigh about 1000 lbs. The surfaces were ground flat to within 0.001", and holes were drilled and tapped on two inch centers over the entire surface. A 1" x 1" x 5' steel rod was then dogged to one side of the table to serve as a straight edge and reference line for various equipment such as mirror mounts, laser tube holders, etc. All related equipment was designed to a standard height above the table for simplicity and ease of operation.

4.10 Laser Mounts

The original laser tube mounts, shown in Fig. 4.5, were constructed from microscope slide adjusters* fixed to an appropriately designed base and coupled with a collar assembly to firmly hold the glass laser tube. This device provides movement in the horizontal and vertical directions measurable to an accuracy of 0.1 mm. It was thought a device such as this would be necessary to properly align the tube in the Fabry-Perot cavity. Subsequent experimentation proved that movement of the tube was not really necessary (except for the beating experiments as will be explained later), so a simpler and much less expensive mount was designed. A drawing of this

* Purchased from Edmund Scientific Co., Barrington, N. J.

Laser tube mounts with microscope slide adjusters

Figure 4.5

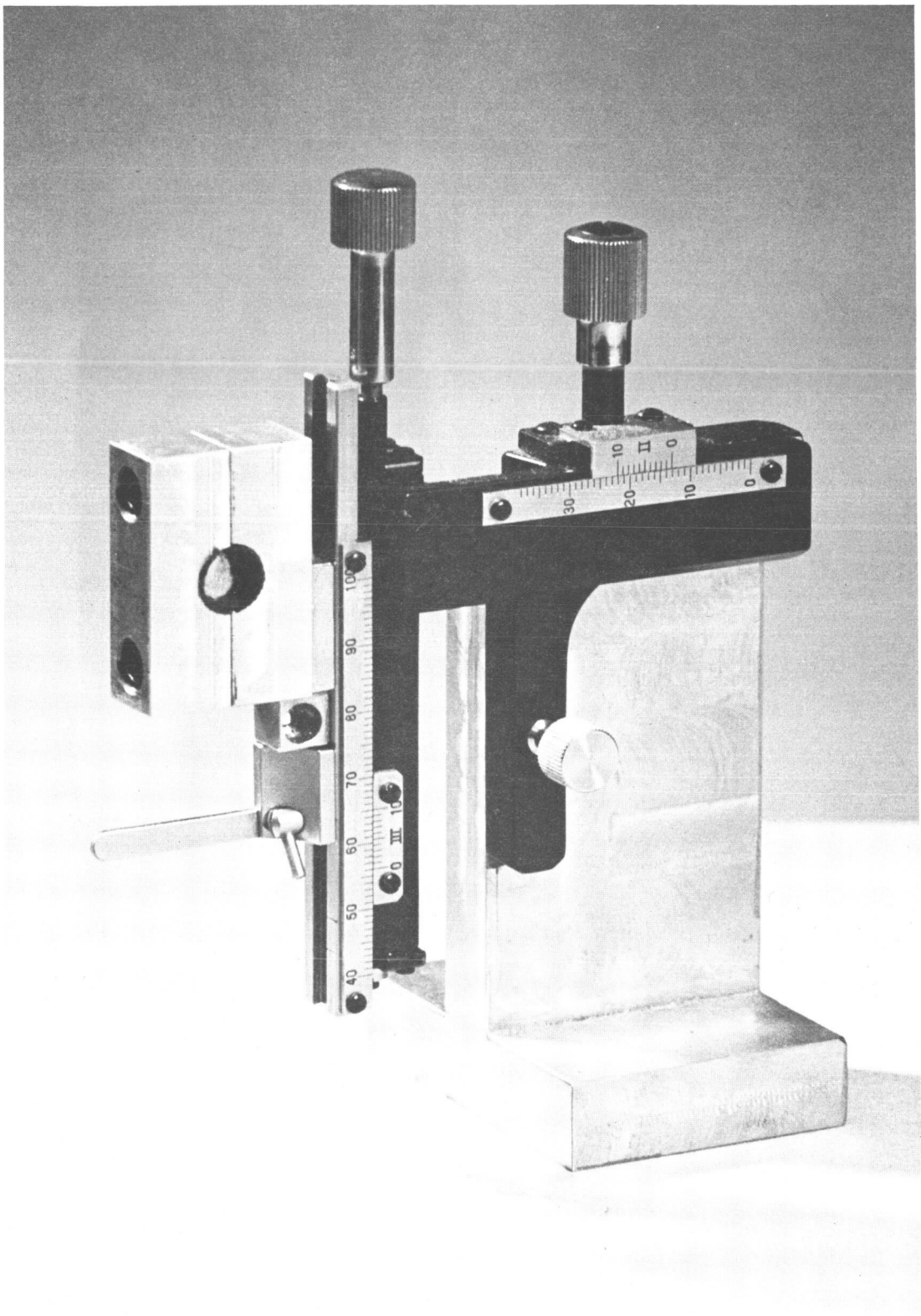
II
10
0
30
20
10
0
III
100
90
80
70
60
50
40

device is shown in Fig. 4.6. An adaptation of this holder was also designed for use on the optical bench which is a part of the vacuum system.

4.11 Mirror Mounts

Three different types of mirror mounts were constructed in the course of this work. The main features of the first two types are illustrated in Fig. 4.7. They were designed to give an angular resolution of 20 seconds of arc, and freedom of movement with a minimum of backlash. The principal difference between the two types is the method of supporting the gimbal axles. The first design utilized a collet as shown in Fig. 4.8; these were expensive to make, and the finished device required a large force to rotate the mirror, putting too much stress on the micrometer head. The improved support utilizes a cone and four-ball bearing as shown in Fig. 4.9; it remedies the defects of the above device. It was found that the amount of accuracy provided by the above mounts is not necessary for most laser experiments. Consequently, a very inexpensive mirror mount of simple design, as illustrated in Fig. 4.10, was constructed and proved to be adequate for most purposes. Fig. 4.11 shows these mirror mounts being used with a 45 cm. laser on the optical bench of the vacuum system.

Inexpensive laser tube holder

Figure 4.6

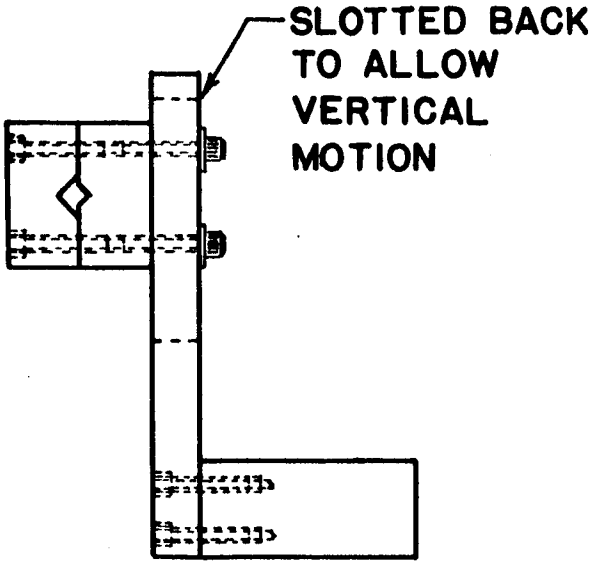
SLOTTED BACK
TO ALLOW
VERTICAL
MOTION

Precision mirror mount

Figure 4.7

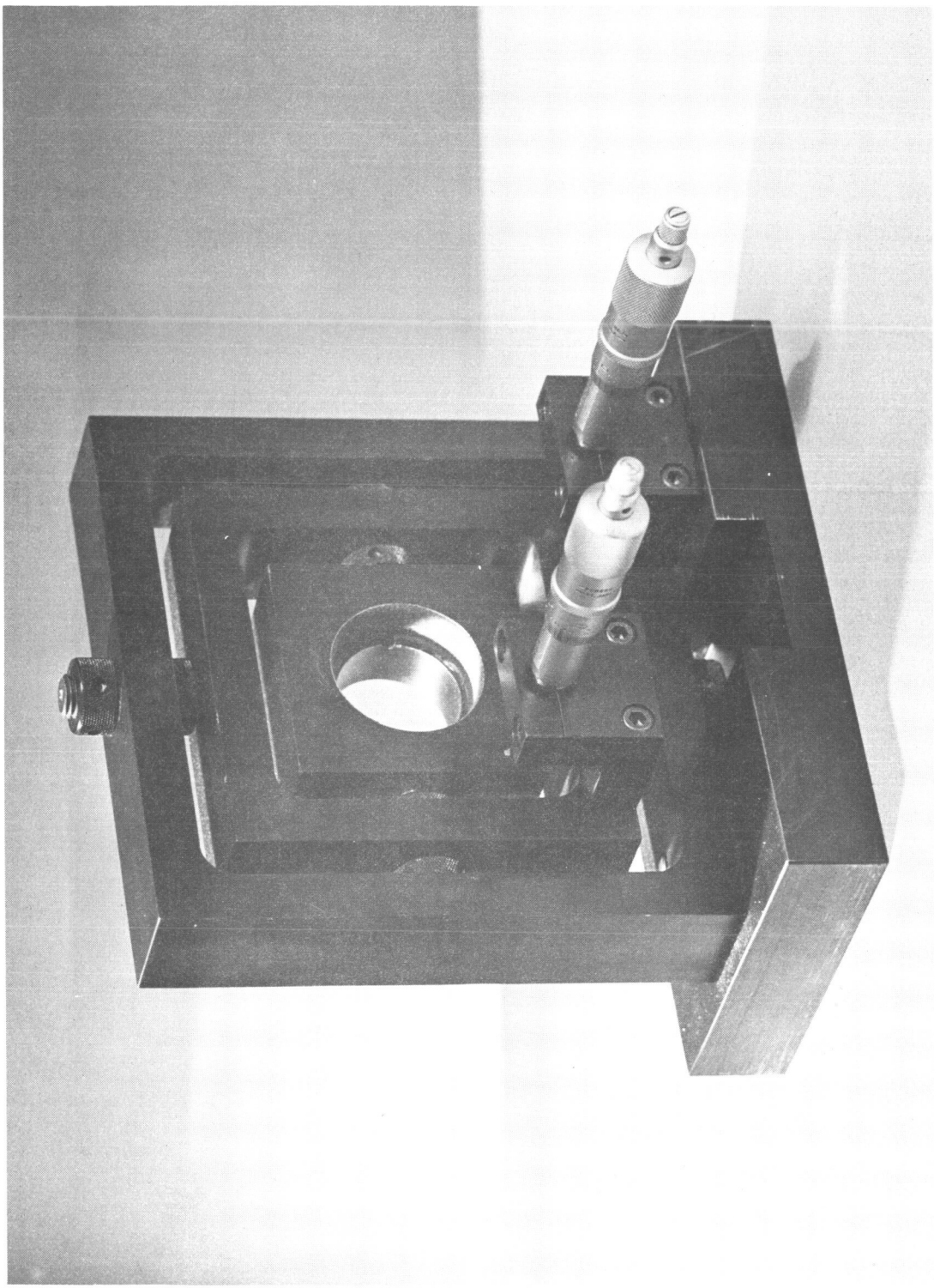

Collet axle support

Figure 4.8

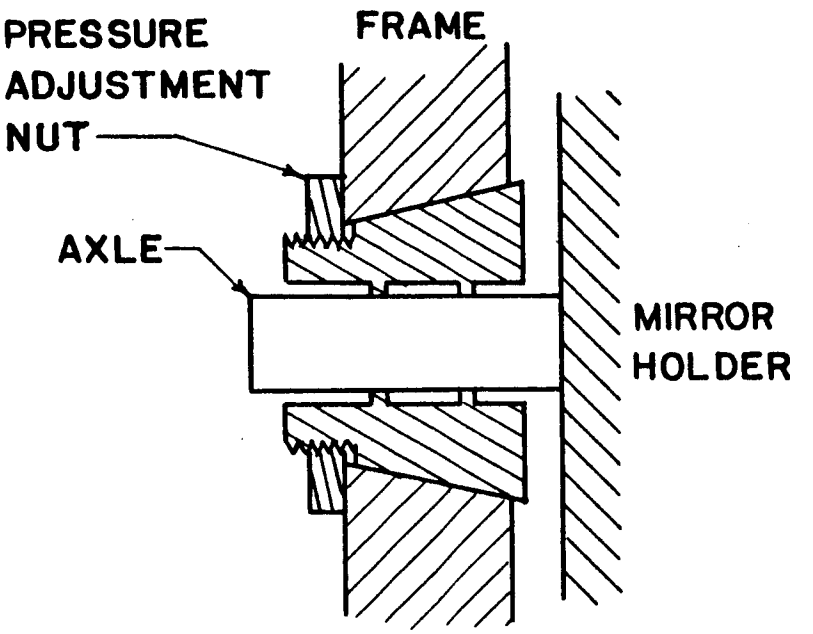
PRESSURE
ADJUSTMENT
NUT
FRAME
AXLE
MIRROR
HOLDER

Cone and bearing axle support

Figure 4.9

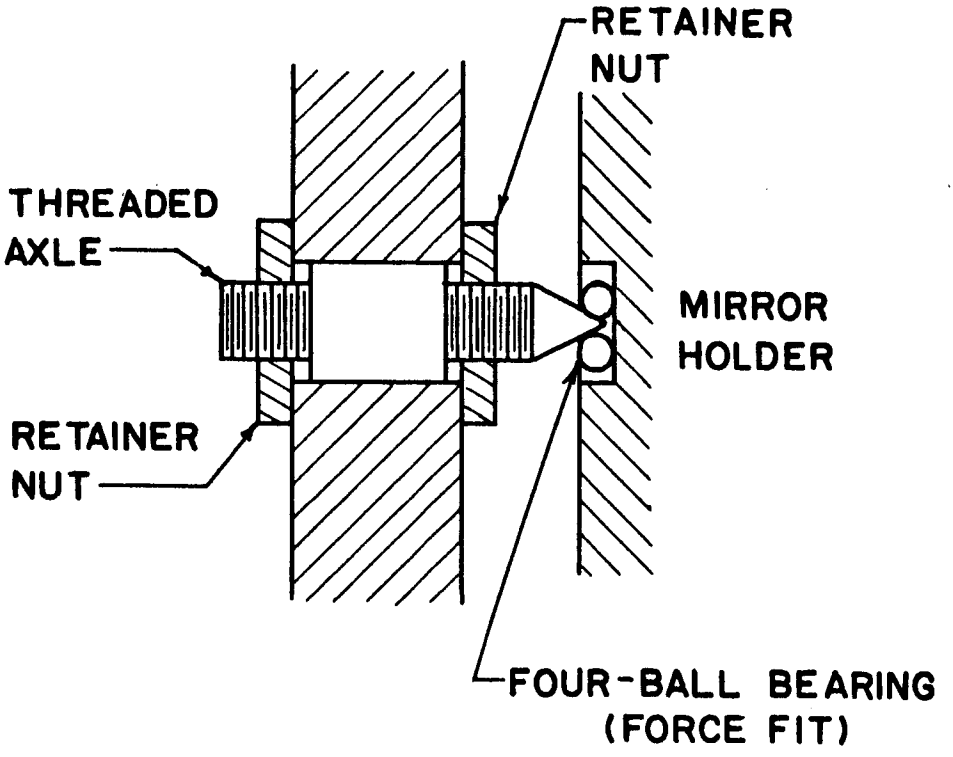
RETAINER
NUT
THREADED
AXLE
MIRROR
HOLDER
RETAINER
NUT
FOUR-BALL BEARING
(FORCE FIT)

Inexpensive mirror mount

Figure 4.10

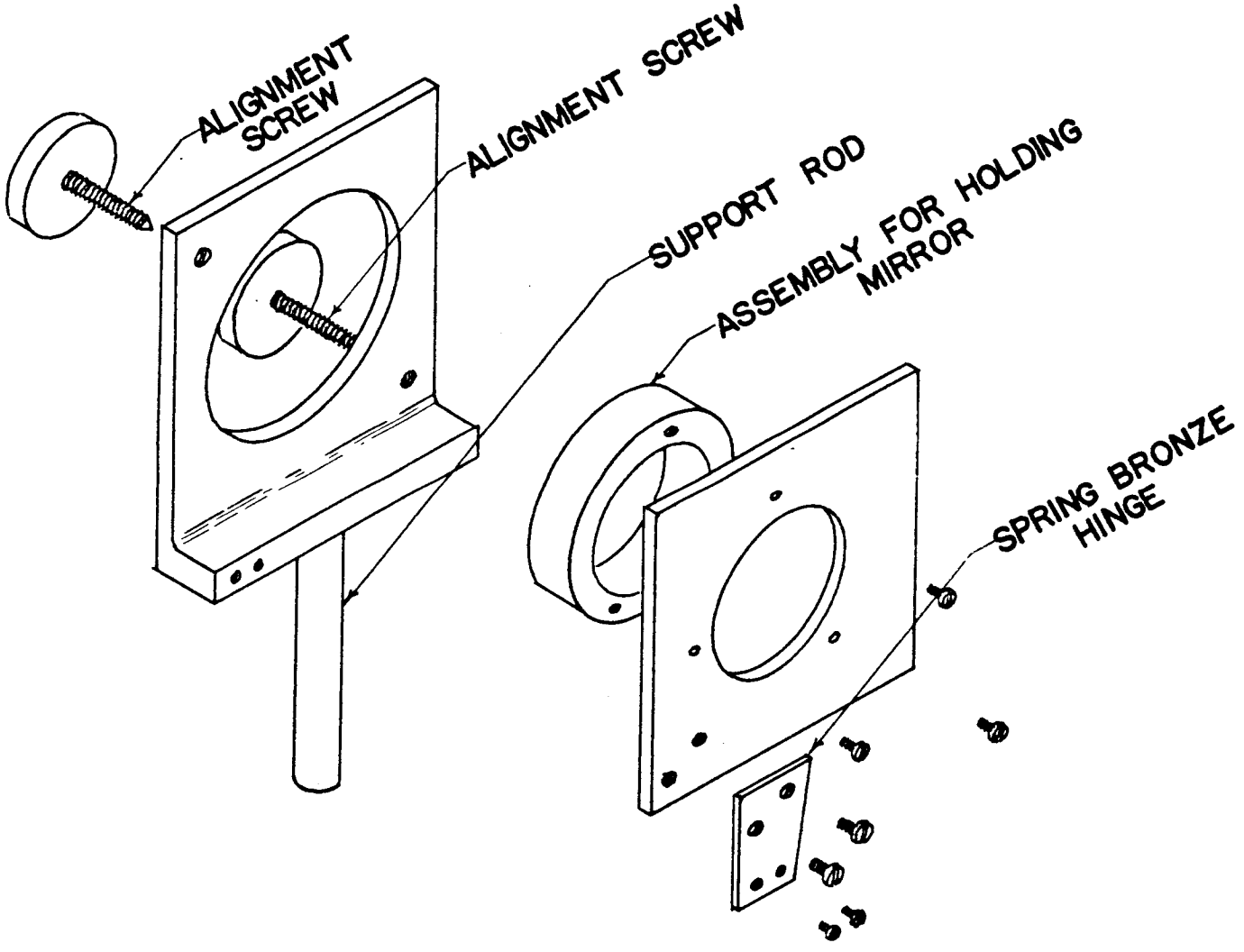
ALIGNMENT SCREW
ALIGNMENT SCREW
SUPPORT ROD
ASSEMBLY FOR HOLDING MIRROR
SPRING BRONZE HINGE

Ten inch laser on vacuum system

Figure 4.11

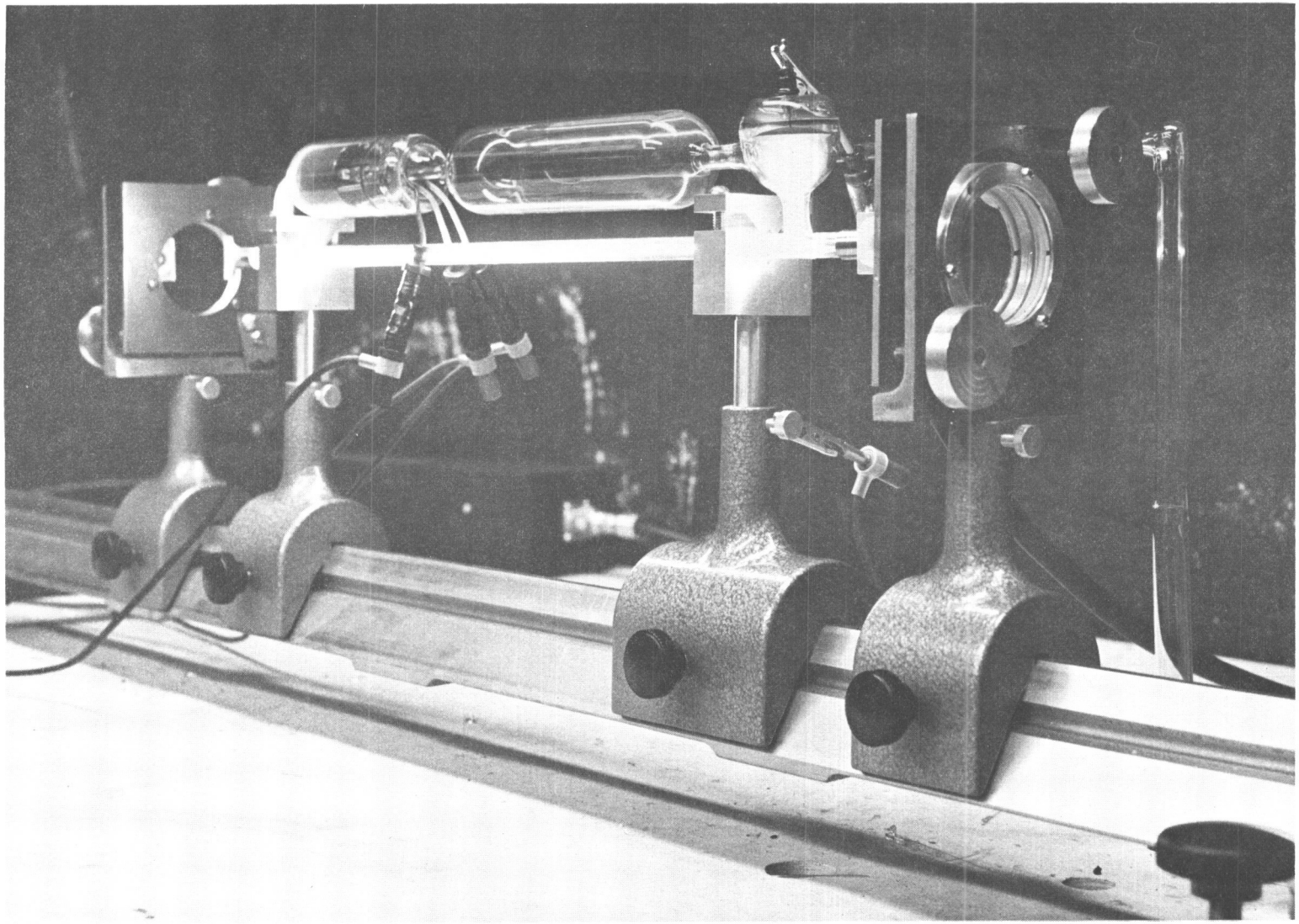

Laser with seven inch active discharge length

Figure 4.12

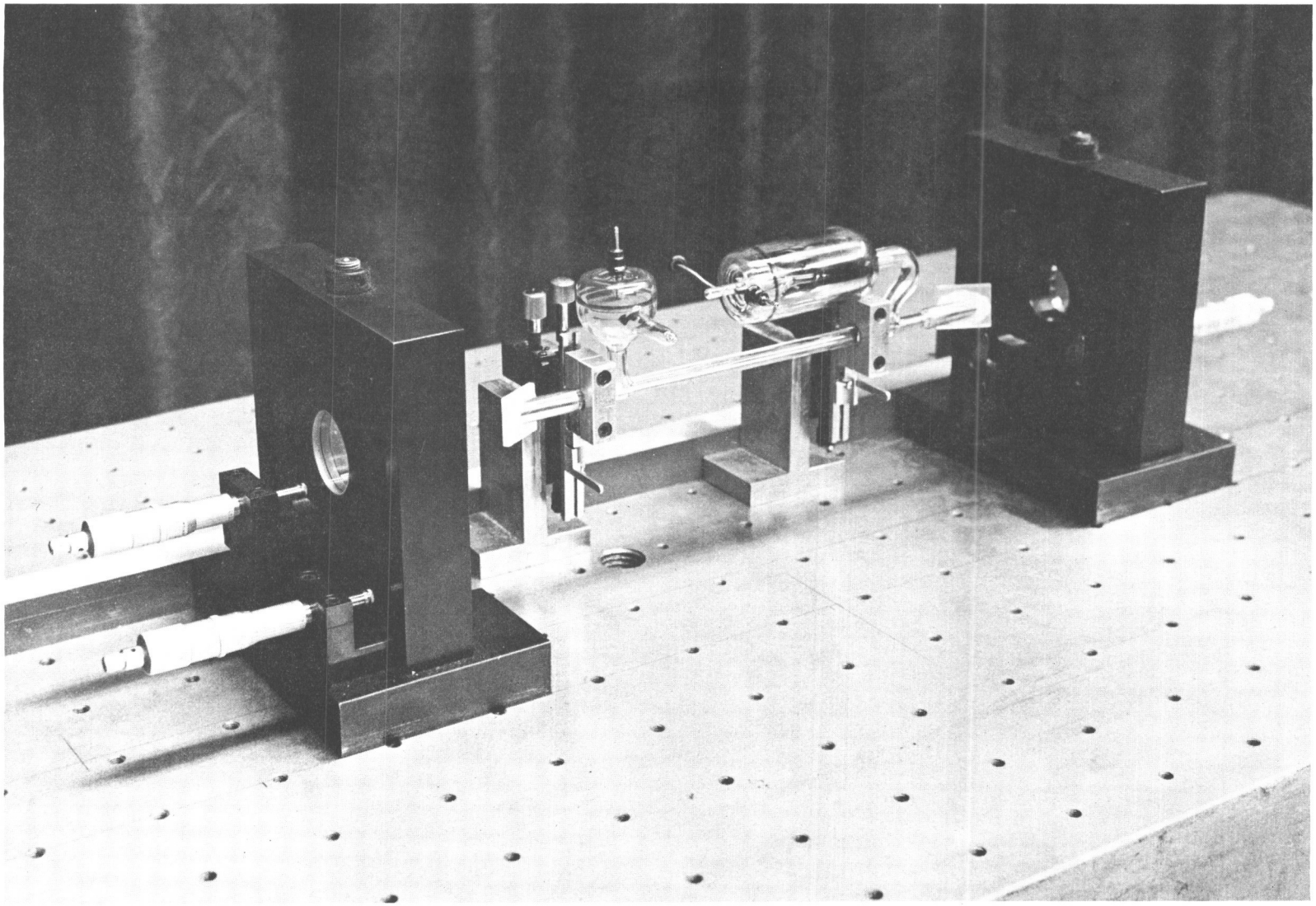

CHAPTER V

OPTICAL HETERODYNING EXPERIMENTS

5.1 Introduction

In this chapter various experimental techniques and associated equipment necessary to obtain beat frequencies between two lasers are discussed. The tolerance on the alignment of the two beams is shown to be very small, and methods of obtaining beam parallelism are described. The results of the beating experiment and sources of frequency drift are reported in detail, followed by an outline of proposed methods to mitigate these drifts.

5.2 Alignment of the Laser Beams

Two requirements must be met in order to successfully obtain beats between two laser outputs: (1) the coherence properties of each laser beam must be maintained, and (2) the light waves incident on the detector must be arranged in such a manner that interference takes place over essentially the entire cross-sectional area of the two superimposed beams. In regard to the first requirement, heterodyning was first attempted using half-silvered mirrors to position the light beams. Their surface quality was sufficiently poor to perturb the coherence of the beams, however, and they did this to the extent that interference necessary to create a beat

frequency could not be obtained. Several high quality beam splitters and prisms were available, and the surfaces of each were tested; the flatness was found to be greater than a wavelength of sodium light per half inch of surface. These were subsequently employed in a beating experiment with good results. Considering the second requirement of superposition of phase fronts, it is possible to compute the approximate angular tolerance between the two beams through the use of elementary interference theory. Envision two plane waves of diameter D, superimposed and incident upon a surface. The condition at which a beat signal is no longer obtained is assumed to be as shown in Fig. 5.1. That is, the wave fronts are in phase on the left while the distance between them on the right side is $\lambda/2$. It is easily shown, using well known approximations, that the angle θ between the normals to the wave fronts is given by $\theta = \lambda/2D$. Since the variation may be + or -, the total angular tolerance is given by $\theta = \lambda/D$. The beams used in this experiment were masked off by a 1mm diameter pinhole at the phototube; using this for a value of D, θ is found to be approximately equal to two minutes of arc.

Fig. 5.2 shows the geometry of the two lasers used in the first beating attempt. Because of the necessary

Two plane waves of similar frequency incident upon a surface

Figure 5.1

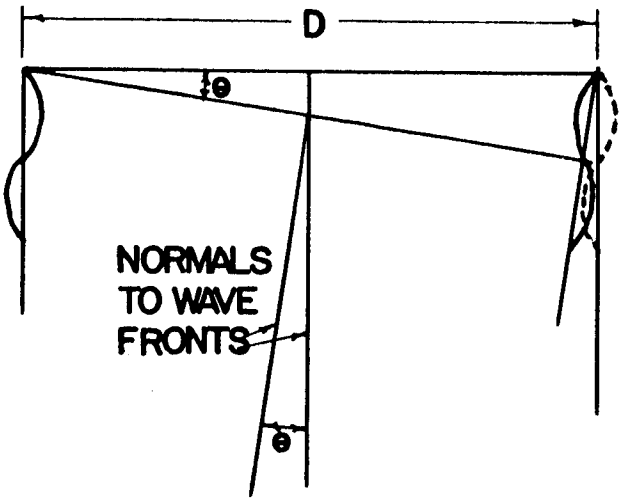
D
θ
NORMALS
TO WAVE
FRONTS
θ

Laser geometry in first beating experiment

Figure 5.2

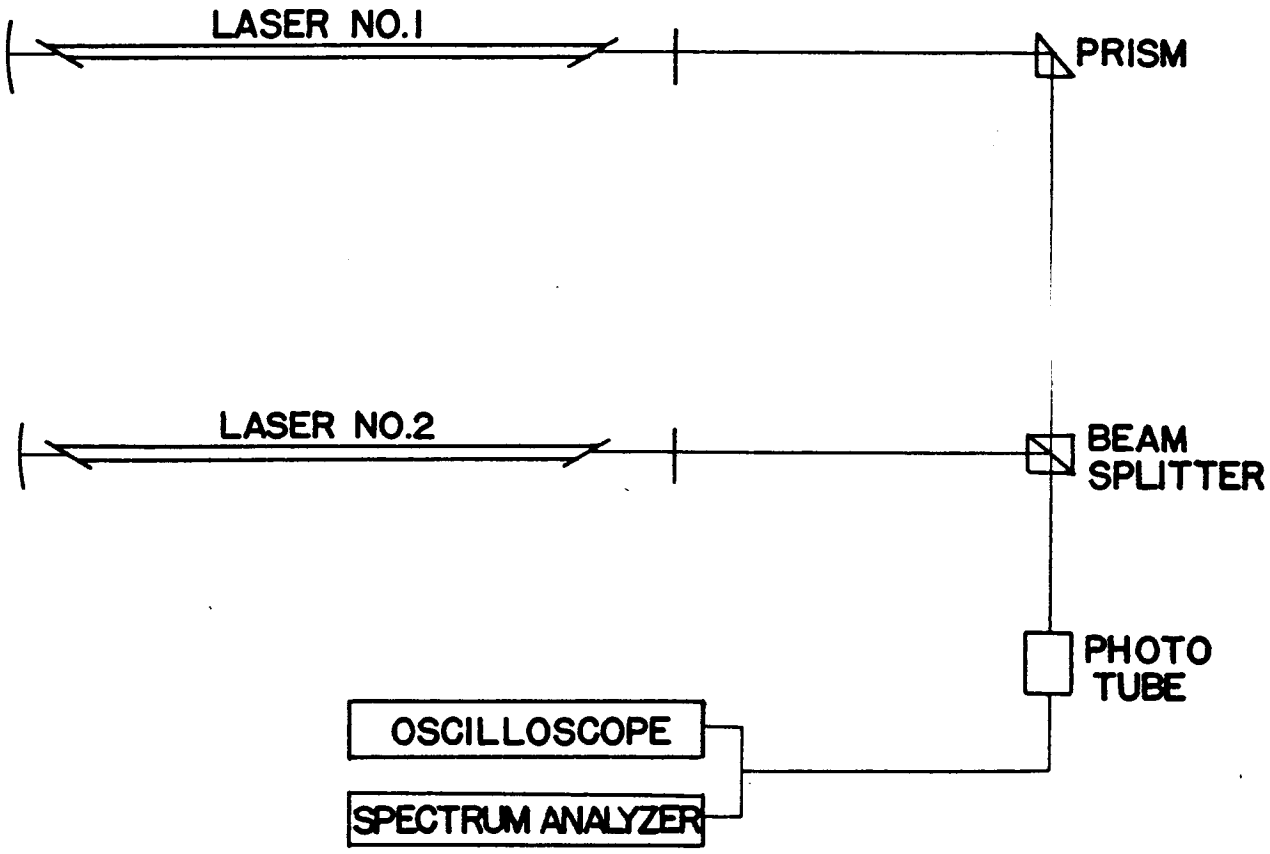
LASER NO.1
PRISM
LASER NO.2
BEAM
SPLITTER
PHOTO
TUBE
OSCILLOSCOPE
SPECTRUM ANALYZER

precision, superposition of the two laser beams on the detector was found to be a very tedious and time-consuming process. The most efficient method of alignment found is described as follows: The lasers are made parallel by allowing the beams emitted from each end of the tubes to fall on opposite walls of the room. The distance between the beams and their height above the floor are then made the same on each wall. The beam splitter may now be positioned by setting one face perpendicular to the beam of one laser. This is accomplished by setting the beam reflected from the front surface of the beam splitter (due to normal Fresnel reflection) back onto its source. The prism is now positioned in the other laser beam in a similar manner and set so that the ray of light exiting from it falls on the beam splitter. The two beams are rendered precisely parallel by superimposing them simultaneously at the interface within the beam splitter and at the detector. A final alignment adjustment may be made by monitoring the output of the detector with an oscilloscope or spectrum analyzer while moving laser number two or the beam splitter.

A second laser geometry is shown in Fig. 5.3. In this system a laser and beam splitter are set up so that

Laser geometry in second beating experiment

Figure 5.3

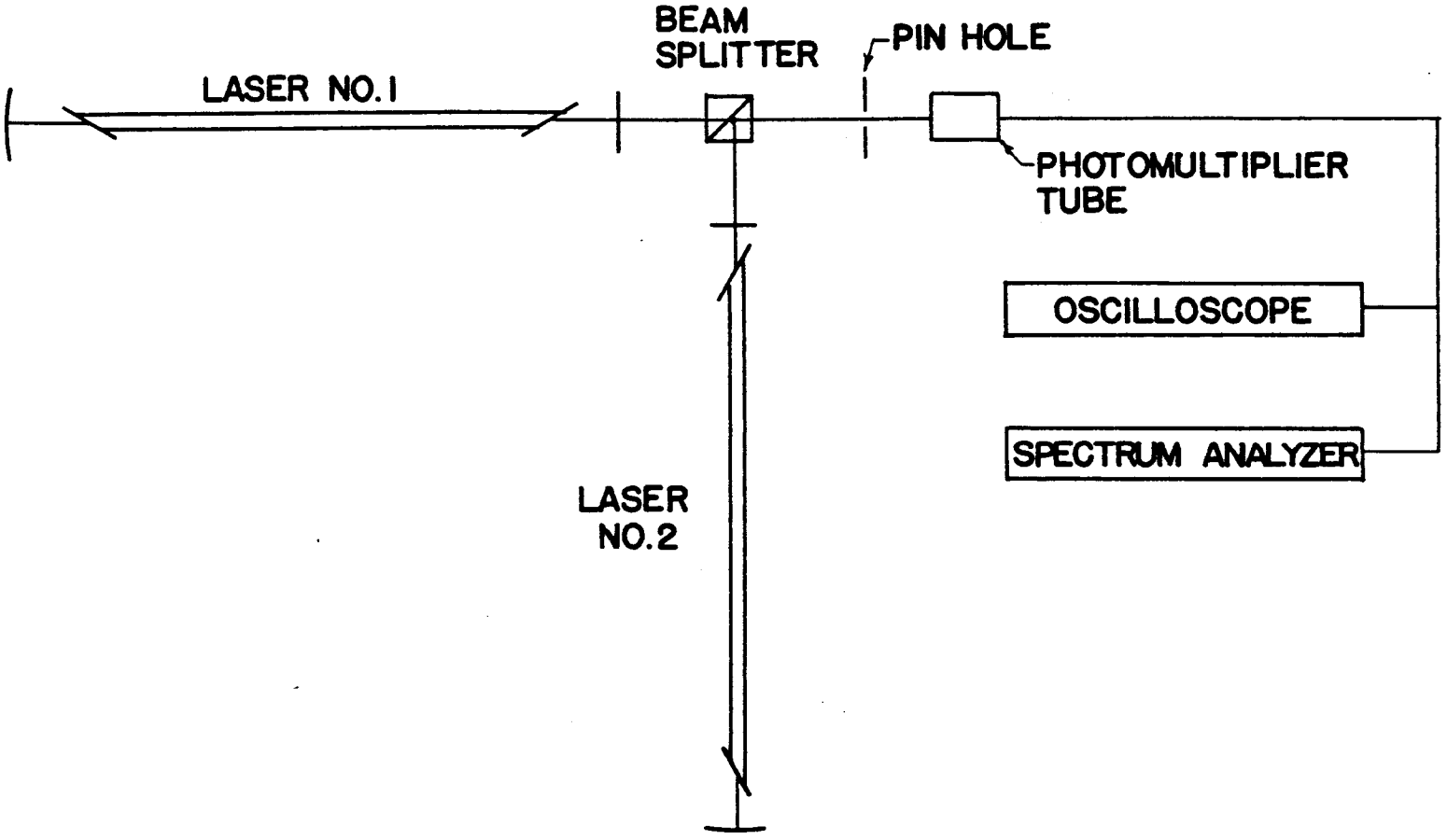
BEAM
SPLITTER
PIN HOLE
LASER NO.1
PHOTOMULTIPLIER
TUBE
OSCILLOSCOPE
SPECTRUM ANALYZER
LASER
NO.2

the beams incident upon and transmitted by the beam splitter are perpendicular as described above. The second laser is then positioned so that its beam is coincident with that of the other at both the interface of the beam splitter and at card A. Two advantages of this system over the first are the ease of alignment, and the decrease in distortion of the spatial coherence of one of the beams by elimination of the prism. This system gave a much more stable beat frequency than that obtainable with the one previously described. It should be noted, however, that in the former system the two lasers were placed on one optical bench, while the prisms, beam splitters, and photo multiplier tube were placed on another. It is entirely possible that this separation added to the instability.

5.3 Detection of the Beat Frequency

An RCA 6655A photomultiplier tube was used to detect the frequency difference between the two lasers. It proved adequate over the frequency range encountered- 0 to 50 Mc/s, the limit of the spectrum analyzer used. No tests were made to determine its maximum frequency response. An attempt was initially made to use a 1P42 photo tube to take advantage of its frequency response characteristics, however, the output of the tube proved to be too small.

The difference in diameter of the two laser beams represents superfluous radiation and, in effect, produces noise in the photo-multiplier tube. If a pinhole is placed in the beam, it will mask out the unwanted portion of the light and reduce the noise considerably.

5.4 Causes of Beat Frequency Drift

Three phenomena are primarily responsible for the frequency drift associated with the beating experiment: (1) mechanical vibration, (2) temperature fluctuation, and (3) change of index of refraction of the media within the cavity. Each of these acts in some way to change the optical length of the cavity. To reduce the effects of mechanical vibration, the equipment was set up on the approximately 1000 lb., 2 1/2' x 5' optical bench described in Chapter IV. Each of the three legs was isolated from the floor by 3/8 in. thick rubber shock mounting pads for the first trials. The beat frequency of the first few runs was very unstable and varied in a more or less random fashion, as indicated by the spectrum analyzer. A vacuum pump was running continuously in the same room at the time, but turning it on and off had no observable effect on the beat frequency stability. The principal cause of instability is thought to be a warping of the table top caused by motion of the floor. This hypothesis seems to be val-

idated by the following observations: The frequency was much more stable around one or two o'clock in the morning, when the building was empty, than it was in the middle of the afternoon. It was possible to change the beat note by more than 30 Mc/s (the frequency range of the spectrum analyzer) by simply applying a slight pressure, to any point on the table top. The frequency could also be changed by walking around the laser table. Because of these results, an effort was made to refine the shock mounting of the table. Each leg was placed on a 1/2 in. thick plywood sheet separated from the floor by an ordinary automobile tire inner tube. This improvement resulted in a substantial increase in beat frequency stability. Only the laser configuration shown in Fig. 5.3 was tested with this type shock mount.

Fig. 5.4 shows an oscilloscope trace of the beat frequency of two lasers obtained with the arrangement shown in Fig. 5.2. A qualitative indication of the stability may be gained from it. Near the end of the second centimeter in the photograph, the jitter due to a shifting frequency is about 2mm wide. This is indicative of 10% drift in the 7.5 Mc/s frequency (the oscilloscope sweep speed was 2m sec/cm) over a period of 40 msec, the exposure time of the picture. An oscilloscope trace of the beat obtained with the improved

Oscilloscope Trace Showing Beat Frequency

Figure 5.4

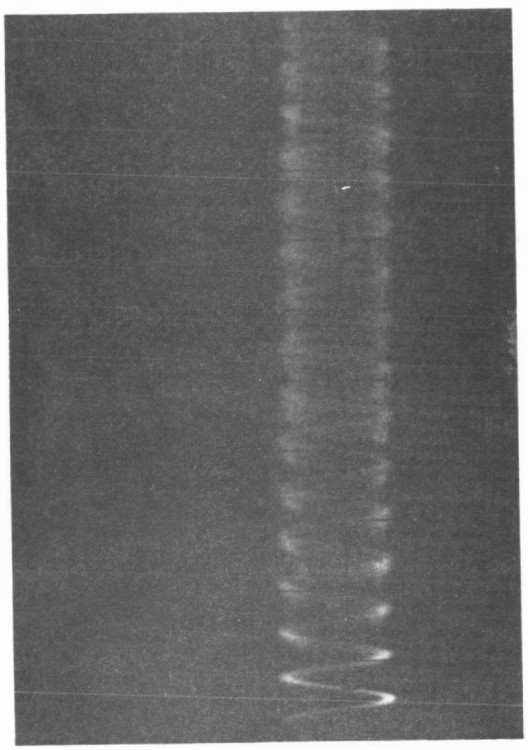

shock mounting revealed an approximate 10% shift of a 2Mc/s frequency over a period of 1/2 sec. Unfortunately, the picture is not suitable for reproduction and time did not allow for a rerun of the experiment. In still another instance, the beat frequency was held at 30 ± 2 Mc/s for 10 sec by applying pressure at a convenient spot on the top of the laser table. The best observed stability is estimated to be a drift 50 Kc/s over a period of 1 sec.

Very little work was done to determine experimentally the effects of temperature fluctuations on frequency stability. From the theoretical analysis given in Chapter II, it is easily seen that a small change in temperature gives rise to a large change in frequency. However, because of the nature of the effect, it should be unimportant from the standpoint of short term beat frequency stability.

The other source of instability, the changing of the index of refraction of the air within the cavity, is due chiefly to air currents. By merely breathing into the cavity or waving a hand nearby to cause drafts, one can alter the frequency. To frustrate this phenomenon, the Brewster's angle windows were placed as close as possible to the mirrors.

5.5 Proposals for Improvement of Beat Frequency Stability

In summary then, beat frequency drift is primarily the result of a variation in light path within the cavity of one or both lasers. It may be brought about by actual mechanical motion of the mirror mounts or a change in the index of refraction of the air within the cavity.

Various ideas have been extended either to eliminate or compensate for these factors. Since the index of refraction is affected chiefly by air currents, the region between the Brewster's angle windows and the mirror could be completely enclosed or perhaps even evacuated to reduce this effect.

The diagram in Fig. 5.5 represents a possible scheme to reduce the effects of temperature and some modes of mechanical vibration on the mirror separation. Since the relative frequency shift between the two lasers causes the beat frequency drift, no beat frequency drift will be evident if both lasers are made to shift in frequency simultaneously and in equal amounts. In this proposal, the laser tubes on individual laser tube mounts, are arranged parallel to one another with their tube centers one inch apart. Both are then aligned with reference to the common flat mirror, A. Small spherical

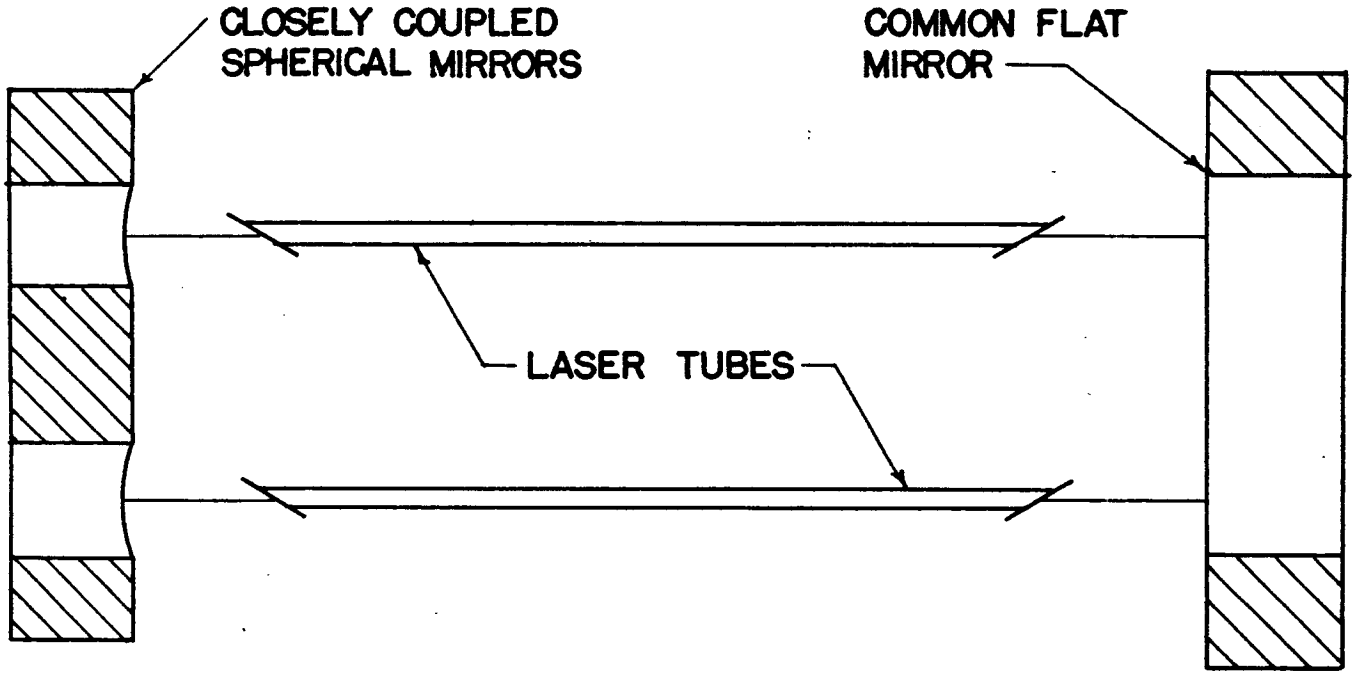
CLOSELY COUPLED
SPHERICAL MIRRORS
COMMON FLAT
MIRROR
LASER TUBES

Proposed device to inhibit beat frequency drift

Figure 5.5

mirrors B and C are fitted into a precisely machined block such that their respective lines, perpendicular to the reflecting surface at the center of the mirror, are accurately parallel. The small adjustments now necessary to allow the tubes to lase may be made by altering the position of the spherical mirror mount, either tilting it slightly or shifting it laterally as determined by experiment. If now mirrors B and C or mirror A are moved perpendicular to their surface by vibration or temperature variation, the change in length of each cavity will be identical.

Another method of reducing the adverse effects of vibration is to reduce the vibration itself. This may be achieved to a certain extent by mounting the equipment on a table set in the bedrock of the earth or in a deep cellar. Though such a facility is available, no attempt has been made to test its usefulness.

CHAPTER VI

CONCLUSIONS AND RECOMMENDATIONS FOR FURTHER STUDY

6.1 Conclusions

Concerning the beating experiments, it has been shown that very small changes in mirror separation result in substantial changes in output frequency of a laser. Hence an optical heterodyne system is profoundly influenced by such environmental factors as vibration and temperature change. Without a great expenditure of effort, however, these deleterious factors can be reduced to the point where, at least, the probing of a plasma on a pulsed basis becomes physically realizable. The best results obtained in the above described heterodyning experiments showed a frequency drift of approximately 50 kc/s over a period of 1 sec. A frequency shift of the same magnitude will be produced by a plasma electron density of 10^{12} electrons/cc; of course the time of formation of the plasma will generally be much shorter than a second. The effects of mode pulling have been shown analytically to give rise to, in some cases, a sizable correction factor to electron density measurements. Some experimentation is necessary in this area to insure that the actual frequency corrections conform to theoretical calculations.

In the process of developing and constructing the lasers necessary to this project, several interesting facts have emerged. Among the most significant is that a gaseous helium-neon laser can be built very inexpensively (estimated to be less than $300, excluding the cost of the mirrors and the power supply) once the techniques for constructing them have been established. It has also been found that some of the component parts do not have to meet the rigid specifications implied by the current literature concerning these devices. Specifically, the Brewster angle windows may be mentioned; very high quality optically flat quartz windows were used on some of the early lasers. Later, government surplus optical flats were found to work equally as well. It was also found that various tolerances, especially on window angles, are not as stringent as once thought. Thus, though lasers are still not simple to construct, they are by no means as exacting and complicated as the original model built by Javan et al.[15, 20]

6.2 Recommendations for Further Study

In the course of this study many questions were raised which still remain unanswered, and several techniques of laser construction are still open to refinement. Perhaps one of the most puzzling phenomena encountered

which could be studied is the effect of the ballast tube on laser action. At times a glow with the characteristic color of the excited helium-neon gas, though much less intense than the main discharge, would appear in the ballast tube. When this occured, laser action was measurably decreased or sometimes even extinguished although no visible change in the discharge between the cathode and the anode took place.

In the realm of the beating experiments, of course, a great deal needs to be done. Methods must be improved for isolating equipment from environmental distrubances or alternately to render these disturbances ineffective in perturbing the beat frequency. Particularly, means must be found to compensate for or eliminate vibration and temperature changes. Also, the effects of mode pulling on frequency shift must be experimentally investigated.

Several aspects of laser tube construction can certainly be improved in order to increase the life of the tube. The method of attaching the Brewster angle windows to the laser tube by epoxy resin is not entirely satisfactory. The epoxy is subject to minute leaks which allow air to enter the tube; it also deteriorates rapidly at temperature above 90° C. The oxide-coated cathode leaves much to be desired as an electron emitter.

Sometimes the coating flakes off and settles on the Brewster angle windows; eventually the gain is diminished until laser action can no longer occur.

REFERENCES

1. L. Spitzer, Jr., Physics of Fully Ionized Gasses (Interscience Publishers, Inc., New York, N. Y.; 1956)

2. D. E. T. F. Ashby and D. F. Jephcott, Appl. Phys. Letters 3, 13 (1963)

3. J. B. Gerardo and J. T. Verdeyen, Appl. Phys. Letters 3, 121 (1963)

4. P. G. R. King and G. J. Steward, New Scientist 17, 130 (1963)

5. A. Javan, Production and Applications of Optical Maser Action Using a Gaseous Discharge, Third annual meeting of the division of Plasma Physics, American Physical Society, Colorado Springs, Colo. (Nov. 1961)

6. T. S. Jaseja, A. Javan, C. H. Townes, Phys. Rev. Letters 10, 165 (1963)

7. T. S. Jaseja, A. Javan, J. Murray, and C. H. Townes, Phys. Rev. 133, 1221 (1964)

8. B. M. Oliver, Proc. I. R. E., 49, 1960 (1961)

9. U. R. Spangenberg, Fundamentals of Electron Devices (McGraw-Hill Book Co., Inc., New York, 1957), P. 464

10. W. R. Bennett, Jr., Phys. Rev. 126, 580 (1962)

11. W. R. Bennett, Jr., Appl. Opt. Suppl. on Opt. Masers, 24 (1962)

12. A. D. White and J. D. Rigden, Proc. I. R. E. 50, (1962)

13. E. I. Gordon and A. D. White, Appl. Phys. Letters 3, 199 (1963)

14. A. D. White and E. I. Gordon, Appl. Phys. Letters 3, (1963)

15. A. Javan, W. R. Bennett, Jr., and D. R. Herriott, Phys. Rev. Letters 6,106 (1961)

16. Douglas C. Sinclair, The Design and Construction of Helium-Neon Visible Lasers (Ph. D. Thesis, The Institute of Optics, The University of Rochester, 1963) Chap. III

17. G. D. Boyd and H. Kogelnik, Bell System Tech. J. 41, 1347 (1962)

18. J. P. Goldsborough, J. Appl. Opt. 3, 267 (1964)

19. A. E. Siegman and S. E. Harris, Proceedings of the Symposium on Optical Masers, ed. Jerome Fox (Polytechnic Press, Booklyn, N. Y., 1963), p. 516

20. D. R. Herriott, J. Opt. Soc. of Am. 52, 31 (1962)

BIBLIOGRAPHY

G. Troupe, Masers and Lasers (2nd ed.; John Wiley and Sons Inc., New York, 1963)

J. Fox (ed.), Proceedings of the Symposium on Optical Masers (Polytechnic Press, Brooklyn, N. Y., 1963)

B. A. Lengyel, Lasers (John Wiley and Sons, Inc., New York, 1962)

R. S. Longhurst, Geometrical and Physical Optics (Longmans, Green and Co., LTD., London, 1960)